Abrupt climate changes and the astronomical theory: are they related?

Denis-Didier Rousseau[1,2], Witold Bagniewski[3], and Michael Ghil[3,4]

[1] Geosciences Montpellier, University Montpellier, CNRS, Montpellier, France
[2] Lamont-Doherty Earth Observatory, Columbia University, New York, 10964, USA
[3] Laboratoire de Météorologie Dynamique (Institut Pierre Simon Laplace and CNRS), Ecole Normale Supérieure and PSL University, Paris, France
[4] Department of Atmospheric and Oceanic Sciences, University of California, Los Angeles, CA 90095, USA

Correspondence to Denis-Didier Rousseau (denis-didier.rousseau@umontpellier.fr)

Abstract

Abrupt climate changes are defined as sudden climate changes that took place in tens to hundreds of years or recurred at millennial time scales; they are thought to involve processes that are internal to the climate system. By contrast, astronomically forced climate changes involve processes that are external to the climate system and whose multi-millennial quasi-periodic variations are well known from astronomical theory. In this paper, we re-examine the main climate variations determined from the U1308 North Atlantic marine record, which yields a detailed calving history of the Northern Hemisphere ice sheets over the past 3.2 Myr. The magnitude and periodicity of the ice-rafted debris (IRD) events observed in the U1308 record allow one to determine the timing of several abrupt climate changes, the larger ones corresponding to the massive iceberg discharges labeled Heinrich events (HEs). In parallel, abrupt warmings, called Dansgaard-Oeschger (DO) events, have been identified in the Greenland records of the last glaciation cycle. Combining the HE and DO observations, we study a complex mechanism giving rise to the observed millennial-scale variability that subsumes the abrupt climate changes of last 0.9 Myr. This process is characterized by the presence of Bond cycles, which group DO events and the associated Greenland stadials into a trend of increased cooling, with IRD events embedded into every stadial, the latest of these being an HE. These Bond cycles may have occurred during the last 0.9 Ma when Northern Hemisphere ice sheets reached their maximum extent and volume, thus becoming a major player in this time interval's climate dynamics. Since the waxing and waning of ice sheets during the Quaternary period are orbitally paced, we conclude that the abrupt climate changes observed during the Mid and Upper Pleistocene are therewith indirectly linked to the astronomical theory of climate.

Key words:

Astronomical theory of climate, abrupt changes, Milankovitch, Dansgaard-Oeschger events, Bond cycles, Heinrich events, ice rafted debris, ice sheets, intrinsic climate variability

1 Introduction

Well-dated geological data indicate that the Earth experienced orbitally paced climate changes since at least the late Precambrian – 1.4 billion years ago during the Proterozoic Eon (Benn et al., 2015; Zhang et al., 2015; Hoffman et al., 2017; Meyers and Malinverno, 2018), and all along the Phanerozoic (Lisiecki and Raymo, 2005; Liebrand et al., 2011; Miller et al., 2011; Kent et al., 2017, 2018; Olsen et al., 2019; Drury et al., 2020; Westerhold et al., 2020). These changes reflect the variations in the Earth's axis of rotation – namely in its precession and tilt - and in the geometry of the Earth's orbit around the sun, i.e., in its eccentricity, driven by gravitational interactions within the Solar system (Berger, 1977; Laskar et al., 2011; Hinnov, 2013, 2018). These variations affect the distribution of insolation at the top of the atmosphere, forcing latitudinal and seasonal climate changes with periodicities of tens or hundreds of thousands of years. Although well acknowledged presently in the climate community, this mechanism took a long journey to reach such general acceptance (Imbrie and Imbrie, 1979).

In the 1840s, while visiting Scotland, Agassiz (1842) attributed erratic boulders noticed in the local landscape to former ice age glaciers in the area, recalling his former observations in Switzerland (Agassiz, 1838). Meanwhile, Adhémar (1842) proposed that glaciations, like those inferred by Agassiz from field observations, occurred every 22,000 years, due to the Earth's evolving on an elliptic orbit with its rotation axis tilted with respect to the orbital plane. Adhémar also concluded that, as the Southern Hemisphere receives less solar radiation per year than the Northern Hemisphere (Adhemar was relying on the number of the nights at the boreal pole versus the number of nights at the austral pole), this contributed to keep temperatures cold enough to allow ice sheets to build up.

Five decades later, Croll (1890) presented his theory of the ice ages being driven by the changing distance between the Earth and the Sun as measured on December 21, which is due to the eccentricity of the Earth's orbit and the precession of the equinoxes. He used formulae for orbital variations developed by Le Verrier (1858) and also stated that, above a particular threshold, Northern Hemisphere winters would trigger an ice age, while below another threshold, an ice age would develop in the Southern Hemisphere. According to Croll's theory, it is the slowly evolving eccentricity of the Earth's orbit that is the key driver, with glaciations occurring only when eccentricity is high. He concluded, therefore, that eccentricity can impact the annual amount of heat received from the sun and also leads to differences in seasonal temperatures.

Parallel to these physical calculations, observations of frontal moraines in the Alpine valleys led to the identification of numerous glacial events in the past. Considering the geometry and position of the terrace systems resulting from these moraines in Alpine valleys, Penck and Brückner (1909) identified four main glaciations, determined from ice advances in the Alpine foreland: Günz, Mindel, Riss and Würm. This sequence became the paleoclimate framework for many decades, until the development of marine and ice coring programs.

Thirty years after Croll, Milankovitch (1920, 1941), inspired by his exchanges with W. Köppen and A. Wegener, provided a crucial step in advancing the theory that major past climate changes had an astronomical origin resulting from the interaction between the eccentricity of the Earth's orbit around the sun, the precession of the equinoxes, and the tilt of the Earth's rotation axis. This theory, often given today his name, implies a fairly regular, multi-thousand–year variability. Based on this crucial idea and on using the recent orbital calculations of Pilgrim (1904), among others, Milankovitch was able to estimate temperatures and insolation at various

latitudes at the top of the atmosphere and to follow their variations through time. Among the results of these estimates, he found that the summer insolation at 65°N is best correlated with glacial–interglacial transitions, as determined by Penck and Brückner's (1909) study of Alpine glaciations.

Milankovitch's astronomical theory of climate was severely criticized by contemporary physicists and rejected by most Quaternary geologists as isotopic C^{14} dating threw the Günz-Mindel-Riss-Würm classification out the window (e.g., Flint, 1971), and references therein). Interest in this theory was restored, however, as the pace of Quaternary climate changes — defined now by $\delta^{18}O$ records from benthic foraminifera (Emiliani, 1955) — was connected on a much sounder basis with orbital variations in the seminal paper of Hays et al. (1976). At the same time, Berger (1977, 1978), using the much more accurate orbital calculations of Chapront et al. (1975), linked more reliably the insolation variations to the waxing and waning of the huge Northern Hemisphere ice sheets over North America, Greenland, Iceland and Europe, including the British Islands and Fennoscandia. The Quaternary period, however, also shows an intriguing transition between the 40 kyr cycles that is dominant during the Early, or Lower, Pleistocene, i.e. from 2.6 Ma up to 1.25 Ma, and the dominant 100-kyr cycles of the Mid- and Late, or Upper, Pleistocene, i.e. the last 800 kyr that show longer glacials implying much larger continental ice sheets. The transition interval, between 1.25 Ma and 0.8 Ma, named the Mid-Pleistocene Transition (MPT: Pisias and Moore, 1981; Ruddiman et al., 1989), experienced variability that does not appear to be directly linked to insolation changes at high latitudes. In fact, the processes involved are not fully understood and still a matter of debate (Ghil & Childress, 1987, Sec. 12.7; Ghil, 1994; Saltzman, 2002; Clark et al., 2021).

Although the broad astronomic framework for past climate changes seems to be widely accepted, high-resolution investigations over the past decades in ice, marine and terrestrial records revealed much shorter periodicities than the orbital ones, as well as abrupt changes that do not match the transitions attributed to variations in eccentricity, obliquity, or precession of the equinoxes. This millennial variability, identified initially during the last climate cycle (Dansgaard et al., 1982), has been described in older records indicating that it prevailed during at least the past 0.5 Ma, as recorded in marine records (McManus et al., 1999). The increased resolution of these records has shown that millennial climate variability can be observed in all types of records, including in ice (Johnsen et al., 2001; Buizert et al., 2015a), marine (Broecker, 2000; Shackleton et al., 2000) and terrestrial (Sanchez-Goni et al., 2000, 2002; Cheng et al., 2016) records associated with abrupt warmings or with strong, and massive, iceberg discharges into the North Atlantic Ocean (Ruddiman, 1977; Bond et al., 1992, 1993; Andrews and Voelker, 2018) that correspond to particular cooling events. Both hemispheres have been impacted by this millennial variability through a mechanism described as the bipolar seesaw (Stocker and Johnsen, 2003).

In this paper, we show that abrupt climate changes are still affected, albeit indirectly, by changes in insolation and hence in overall ice sheet volume. In this sense, the Milankovitch framework is shown herein to be quite relevant to the study of abrupt and large climate changes. The paper is organized as follows. In Sec. 2, we describe the records and the methods used to identify the major transitions. In Sec. 3, major transitions for the last 3.2 Myr of Northern Hemisphere climate are described. In Sec. 4, we concentrate on the millennial-scale variability revealed by these records. In Sec. 5, we establish a connection between Dansgaard-Oeschger (DO)

events and amended Bond cycles, and outline how global ice sheet volume affects the latter. Concluding remarks follow in Sec. 6.

2 Material and methods

2.1 The records

Over the past 66 Myr, corresponding to the Cenozoic Era, Earth's climate has experienced four main states, from "Warmhouse" and "Hothouse," between 66 Ma and 34 Ma, to "Coolhouse" and "Icehouse," from 34 Ma until the present time; see Fig. 1a. Although the first two states alternated in a warm-hot-warm sequence, the last two succeeded each other, thus generating the classical climate trend towards the recent ice age conditions (Zachos et al., 2001; Westerhold et al., 2020; Scotese et al., 2021). The last 3.3 Myr have been defined as an Icehouse climate state, with the appearance of the Northern Hemisphere ice sheets and their variations through time (Westerhold et al., 2020). This Icehouse state is characterized by a change of the interplay between benthic $\delta^{13}C$ and $\delta^{18}O$, which corresponds to a new relationship between the carbon cycle and climate. Indeed, the negative excursions in $\delta^{13}C$ were associated with negative ones in $\delta^{18}O$ during most of the Cenozoic since 66 Ma. A shift occurred, though, in the Plio-Pleistocene, at about 5 Ma, with negative $\delta^{13}C$ excursions being associated with positive $\delta^{18}O$ ones (Turner, 2014). Such a shift appears to be related to a dichotomy in the response of the marine and terrestrial carbon reservoirs to orbital forcings.

The past 3.2 Myr of Northern Hemisphere climate are particularly well described in North Atlantic core U1308 at (49.87N, 24.24W) (Hodell and Channell, 2016). This core is located in the ice-rafted debris, (IRD) of continental detrital material eroded by the ice sheets (Ruddiman, 1977), and it yields a more complete record than U1313 (Naafs et al., 2013); see Fig. 1b. The variations in the benthic $\delta^{18}O$ mostly indicate varying periodicities through time that correspond to periodicities in the orbital parameters of Earth's climate (Hodell and Channell, 2016; see Fig. S1), as confirmed by Lisiecki and Raymo (2005) from the stack oxygen isotope record they produced using 57 marine records from the world's oceans.

The behavior of the U1308 proxy records on the time scale of many tens and hundreds of thousands of years allows us to track the numerous glacial–interglacial cycles of the past 2.75 Myr with the help of variations in Earth's orbital parameters (Fig. S1). Besides these relatively slow variations, evidence of millennial-scale variability can be observed since the appearance of IRD in the North Atlantic at about 1.5 Ma. This much faster variability is superposed upon the classical orbital periodicities; see Fig. 3.

Observations of such abrupt variations have been reported in some detail for the last glacial period by the North Greenland Ice Core Project at (75.1N, 42.32W) (Barbante et al., 2006). The $\delta^{18}0$ record best describes the more or less regular recurrence of cold and warm events that we are analyzing; see Fig. 1c.

2.2 The methods

The increase in resolution of the Greenland ice cores (Fischer et al., 2015; Schupbach et al., 2018; Svensson et al., 2020) and of several speleothems (Cheng et al., 2016) allowed one to conduct much more detailed analyses of the $\delta^{18}O$ but also of other proxies, such as dust content, leading to the identification of sub-events, as compiled by Rasmussen et al. (2014). It is these high-resolution analyses that led to defining the Greenland Interstadials (GIs), followed by the associated Greenland Stadials (GSs). To gain further insight into the climate

story the records tell us, we performed a quantitative, objective analysis of these time series of proxy variables, based on two methods: the Kolmogorov-Smirnov (KS) augmented test of Bagniewski et al. (2021) and the recurrence plots (RPs) of Marwan et al. (2007, 2013).

Bagniewski et al. (2021) proposed a method based on an augmented nonparametric Kolmogorov-Smirnov (KS) test to efficiently and robustly detect abrupt transitions in paleo-records. The classical KS test consists of quantifying and comparing the empirical distribution functions of two samples from a time series, before and after a potential jump. In the present case, the test is augmented by varying window sizes and by evaluating the rate of change and the trend in maxima and minima of the time series. This method allows one to reliably establish the main transitions in a record, such as the marine isotope stages in the SU 1308 benthic δ^{18}O or the GS–GI boundaries in the North Greenland Ice Core Project (Barbante et al., 2006) δ^{18}O.

The recurrence plots (RPs) were introduced by Eckmann et al. (1987) into the study of dynamical systems and popularized in the climate sciences by Marwan et al. (2007, 2013). The purpose of RPs is to identify recurring patterns in a time series in general and in a paleoclimate time series in particular.

The RP for a time series $\{x_i: i = 1, \dots, N\}$ is constructed as a square matrix in a cartesian plane with the abscissa and ordinate both corresponding to a time-like axis, with one copy $\{x_i\}$ of the series on the abscissa and another copy $\{x_j\}$ on the ordinate. A dot is entered into a position *(i, j)* of the matrix when x_j is sufficiently close to x_i. For the details — such as how "sufficiently close" is determined — we refer to Eckmann et al. (1987) and to Marwan et al. (2013). Clearly, all the points on the diagonal $i = j$ have dots and, in general, the matrix is rather symmetric, although one does not always define closeness symmetrically; to wit, x_j may be "closer to" x_i than x_i is to x_j (Eckmann et al., 1987). An important advantage of the RP method is that it does apply to dynamical systems that are not autonomous, i.e., that may be subject to time-dependent forcing. The latter is certainly the case for the climate system on time scales of 10–100 kyr and longer, which is affected strongly by orbital forcing.

Eckmann et al. (1987) distinguished between large-scale *typology* and small-scale *texture* in the interpretation of square matrix of dots that is the visual result of RP. Thus, if all the characteristic times of an autonomous dynamical system are short compared to the length of the time series, the RP's typology will be homogeneous and, thus, not very interesting. In the presence of an imposed drift, a more interesting typology will appear. The most interesting typology in RP applications so far is associated with recurrent patterns that are not exactly periodic but only nearly so. Hence, such patterns are not that easily detectable by purely spectral approaches to time series analysis. Marwan et al. (2013) discuss how to render the purely visual RP typologies studied up to that point more objectively quantifiable by recurrence quantification analysis and bootstrapping (Efron, 1981; Efron and Tibshirani, 1986).

The selection of the major transitions in the RPs was achieved by performing a recurrence rate (RR) analysis. The values obtained for every record correspond to the mean for different window lengths ranging from 1 kyr to 15 kyr. The selection of the transitions of interest relies therefore on the definition of a threshold that we choose to be the standard deviation of RR prominence, which is 0.089 for the U1308 benthic δ^{18}O, 0.127 for the U1308 bulk carbonate δ^{18}O and 0.173 for NGRIP δ^{18}O. The results were plotted along with the original recurrence plot (Tab. 1). Please see further details in Bagniewski et al. (2021).

3 The Past 3.2 Myr History of the Northern Hemisphere Climate

Analyzing the U1308 benthic $\delta^{18}O$ record allows one to identify the various transitions between the marine isotope stages that covered the last 3.2 Ma and were driven by variations in the orbital parameters (Fig. S1). However, the RPs reveal several key features that appear in the U1308 records during this time interval that are much more plausibly related to processes other than the orbital forcing. Hoddell and Channel (2016) identified four major steps in their climate record. These four steps are linked to thresholds in the benthic and bulk carbonate $\delta^{18}O$ variations, and they occur at 2.75 Ma, 1.5 Ma, 0.9 Ma and 0.65 Ma.

The first date is interpreted as corresponding to the earliest occurrence of IRD in the North Atlantic. This occurrence characterizes the presence of Northern Hemisphere coastal glaciers large enough to calve icebergs into the ocean, and the melting of these icebergs is likely to have impacted the oceanic circulation. Naafs et al. (2013) reported the occurrence of minor IRD events, attributed mainly to Greenland and Fennoscandian glaciers. These events indicate a greater size of ice sheets over these regions than during the later Quaternary, when the North American ice sheets were considerably larger.

The second date corresponds to an increase in amplitude in ice volume variations between glacial maxima and interglacial optima. This second step shows the permanent occurrence of ice-rafted events during glacial intervals in the record. The latter behavior signals a stronger relationship between climate variations and Northern Hemisphere ice sheets.

The third date, close to the MIS22–24 $\delta^{18}O$ optima, shows increased continental ice volume in the Northern Hemisphere (Batchelor et al., 2019), but also more stability in the East Antarctic ice sheet in Southern Hemisphere (Jakob et al., 2020). In parallel, evidence of a major glacial pulse recorded in Italy's Po Plain, as well as in ^{10}Be-dated boulders in Switzerland, is interpreted as marking the onset of the first major glaciation in the Alps (Muttoni et al., 2003; Knudsen et al., 2020). At about the same time, the synthetic Greenland $\delta^{18}O$ reconstruction of Barker et al. (2011), which starts however at 800 ka, indicates the occurrence of millennial variability expressed by DO-like events.

The last date at 0.65 Ma marks the end of the transition from the Lower and Mid-Pleistocene interval — characterized by 41-kyr–dominated cycles and smaller 23-kyr ones — to the Upper Pleistocene, with its 100-kyr–dominated cycles; see Fig. 1b. The sawtooth pattern of the interglacial–glacial cycles (Broecker and van Donk, 1970), which first becomes noticeable at 0.9 Ma, is well established during this final interval, in contradistinction with the previous, more smoothly shaped pattern that appears to follow the obliquity variations. The global ice volume is maximal, exceeding the values observed earlier in the record, especially due to the larger contribution of the Northern American ice sheets. The latter now have a bigger impact on Northern Hemisphere climate than the Eurasian ice sheets (Batchelor et al., 2019). The IRD event intensity and frequency of occurrence increase (McManus et al., 1999) as well, leading to the major iceberg discharges into the North Atlantic named Heinrich events (HEs); see Heinrich (1988), Bond et al. (1992, 1993), and Obrochta et al. (2014). The interval of 1 Ma – 0.4 Ma is also the interval during which Northern Hemisphere ice sheets reached a southernmost extent during MIS16 and 12, similar to the one reached during MIS6 (Batchelor et al., 2019).

The benthic $\delta^{18}O$ record of the U1308 marine-sediment core is interpreted in terms of global ice volume and deep-ocean temperatures (Chappell and Shackleton, 1986; Shackleton, 2000; Elderfield et al., 2012). Its recurrence analysis shows a drift topology (Marwan et al., 2007, 2013) that characterizes a monotonic trend in time, associated with nonstationary systems with slowly varying parameters. The RP exhibits, moreover, a characteristic texture — given by the pattern of vertical and horizontal lines that mark recurrences. These lines sometimes form recurrence clusters that correspond to specific periodic patterns. We thus identify five steps in the $\delta^{18}O$ variability; see Figs. 2a,c, and Tabs. 1 and 2. Two are roughly similar to those determined by Hoddell and Channel (2016): at 1.5 Ma and 0.65 Ma, and three differ: at 2.55 Ma, 1.25 Ma and 0.35 Ma. Interestingly, the interval 1.25 Ma to 0.65 Ma corresponds roughly to the previously mentioned MPT, during which a shift from climate cycles dominated by a 40-kyr periodicity to 100-kyr dominated ones occurred (Shackleton and Opdyke, 1977; Pisias and Moore, 1981; Ruddiman et al., 1989; Clark and Pollard, 1998; Clark et al., 2006). A sixth transition, at 2.95 Ma, is close to the selected threshold, as described at the end of Sec. 2.2.

The $\delta^{18}O$ bulk carbonate record in the U1308 core, in turn, is interpreted as characterizing IRD released into the North Atlantic Ocean, with the most negative $\delta^{18}O$ values representing the largest iceberg calvings (Hodell & Channel, 2016). The recurrence analysis of this record also displays the evolutionary trend represented by a drift topology, and it yields one of the two Hodell & Channel (2016) steps at 1.5 Ma, while the transition at 0.65 Ma is slightly below our threshold (Figs. 3a,c, Tabs. 1 and 2). Our analysis further identifies the steps at 1.25 Ma, 1.65 Ma and 2.75 Ma, with the 1.25 step also noticed in the $\delta^{18}O$. Two other transitions show a recurrence prominence close to our threshold at 1.95 Ma and 2.45 Ma. Table 2, comparing the Hodell & Channel (2016) steps with the thresholds detected by the RP, shows that the former are mainly related to the IRD history of the past 3.3 Ma.

The 1.25 Ma date is particularly significant, since it is followed by an increase in the amplitude of glacial–interglacial fluctuations (Fig. 2a). The interval 2.8 Ma to 1.2 Ma shows glacial–interglacial sea level variations of about 25–70 m below the present-day value (van de Wal et al., 2011). The reconstructed CO_2 concentrations varied between 270 ppmv and 280 ppmv during interglacials and between 210 ppmv and 240 ppmv during glacials, with a decreasing trend of about 23 ppmv over this 1.4-Myr–long interval (van de Wal et al., 2011). After 1.25 Ma, the sea level changes increased to about 70–120 m below the present-day value, while the reconstructed CO_2 concentrations varied between 250 ppmv and 320 ppmv during interglacials and between 170 ppmv and 210 ppmv during glacials (Berends et al., 2021). Similar variations were determined by Seki et al. (2010), although pCO_2 changes that occurred before the time reached by ice core records are associated with high uncertainties in both dating and values. The “Milankovitch glacials,” which correspond to the odd marine isotope stages determined in the U1308 core and in many others, have maxima that are characterized by low eccentricity and obliquity, and a boreal summer that coincides with aphelion and leads, therefore, to minimum values of summer insolation. The increase in IRD variability and magnitude since 1.5 Ma ((Hodell and Channell, 2016), however, shows that distinct, faster processes have to be considered than those due to slow changes in Earth’s orbital parameters; see again Figs. 2 and 3.

4 Millennial-Scale Variability

The behavior of the U1308 proxy records on the time scale of many tens and hundreds of thousands of years was described briefly in the previous section, and it allowed us to track the numerous glacial–interglacial cycles

of the past 2.75 Myr with the help of variations in Earth's orbital parameters; see Supp. Fig. 1. Besides these relatively slow variations, evidence of millennial-scale variability can be observed since the appearance of IRD in the North Atlantic at about 1.5 Ma; this much faster variability is superposed upon the classical orbital periodicities (Fig. 3).

Detailed observations of such abrupt variations have been reported for the last glacial period, with the more or less regular recurrence of cold and warm events; see Fig. 1c. The former are represented by IRD events, some of which are significantly stronger, and represent the previously mentioned HEs that correspond to massive discharges of icebergs into the North Atlantic (Heinrich, 1988; Bond et al., 1992; McManus et al., 1994; Hemming, 2004).

Abrupt warmings happening over as little as a few decades each have been inferred from Greenland ice cores (Dansgaard et al., 1993; Clark et al., 1999), and labeled DOs or Greenland interstadials (GIs: Rasmussen et al., (2014) ; see Fig. 4a. These warm events are followed by a return to glacial conditions, called Greenland stadials (GSs). This return generally happens in two steps, thus forming DO cycles of variable duration that does not exceed a millennial time scale (Broecker, 1994; Boers et al., 2018; Boers, 2018 and references therein). Broecker (1994) do not provide any precise DO timescale but indicates that "climate cycles [average] a few thousands of years in duration". Boers et al. (2018) do not yield any exact value for the DO time scales either, but Figure S1 in their appendix does indicate the durations of the stadials and interstadials in the NGRIP record varying between 340 yr and 8365 yr, and between 190 yr and 16,440 yr respectively.

Numerous DO timescales have been published by Rasmussen et al. (2014), Wolff et al. (2010), Rousseau et al. (2017) and, most recently, Capron et al (2021). However, no DO cycle timescale has been published as yet. Table 3 reports the duration of the DO cycles as expressed by the interval between the start of a GI and the end of a GS as estimated by Rasmussen et al. (2014). It shows that the average duration of a DO cycle is of 4,045 yr ± 3,179 yr. As the periodicity of the events is at millennial and submillennial scale (Broecker, 1994; Clark et al., 1999; Ganopolski and Rahmstorf, 2001; Rahmstorf, 2002; Schulz, 2002; Menviel et al., 2014; Lohmann and Ditlevsen, 2018, 2019), it corresponds to processes that cannot be related to any orbital forcing (Lohmann et al., 2020), but rather to factors that are intrinsic to the Earth System.

DO events were first observed in the various ice cores retrieved from the Greenland ice sheet (Dansgaard et al., 1969; Johnsen et al., 1972). Some of these DOs were correlated to European warm interstadials, which had been described from pollen records (Woillard, 1978; Behre, 1989; Zagwijn, 1989). The existence and dating of the DOs was initially questioned as they had not been observed in marine cores in the 1970s and 1980s (Broecker et al., 1988; Broecker and Denton, 1989). Dansgaard et al (1993), though, clearly identified 23 rapid warming events during the last climate cycle from the Greenland GRIP ice core.

These 23 DO events were later confirmed in other Greenland ice cores (Johnsen et al., 2001), following the initial correlation of rapid changes between Camp Century and Dye3 ice cores (Dansgaard et al., 1982), and they are considered as the "canonical" DOs. They were assigned numbers that increase sequentially downcore, with #1 allocated to the Bølling pollen oscillation (Dansgaard et al., 1993); see Fig. 4a. The 23 canonical DOs were, moreover, described later using various types of records, in marine sediments (Bond et al., 1992; Henry et al., 2016), as well as in terrestrial ones (Allen et al., 1999; Sanchez-Goni et al., 2000, 2002; Müller et al., 2003; Fletcher et al., 2010; Rousseau et al., 2017 a, b, 2021), including speleothems (Wang et al., 2001; Genty et al., 2003; Fleitmann et al., 2009; Boch et al., 2011). The transitions identified by KS test in the NGRIP $\delta^{18}O$

include all the canonical events described by Dansgaard et al. (1993) and identified in Rasmussen et al. (2014), although a few other DOs or subevents are not detected by it, even after changing the test window size; see Fig. S2.

Using a global climate indicator like methane (CH_4) Blunier and Brook (2001), EPICA Community Members (2006) and the WAIS Consortium (2015) demonstrated that the millennial-scale variations observed during the last 130 kyr in Greenland are observed in Antarctica as well, and that they are, therefore, a global phenomenon. Hinnov et al. (2002) also carried out an investigation on the methane-linked GISP2 and Byrd ice cores including a statistically constrained spectral coherency analysis demonstrating the global reach of the DO cycles. The $\delta^{18}O$ variations in the two hemispheres, though, are in opposite phases, with the Southern Hemisphere warmings occurring prior to the Northern Hemisphere ones.

Several hypotheses have been proposed to determine whether the climatic signal propagated between the two hemispheres is in a southward or northward direction. Variations in the Atlantic Meridional Overturning Circulation (AMOC) play a key role in this teleconnection, as AMOC slowdown during GSs corresponds to reduced oceanic northward heat transport (Sarnthein et al., 2001; Ganopolski and Rahmstorf, 2001; McManus et al., 2004). This reduction does not contradict the southward propagation direction of the climate signal, as documented by detailed high-resolution marine-sediment and ice core studies (Buizert et al., 2015b; Henry et al., 2016), with Greenland climate leading Antarctica by approximately 200 years. On the other hand, Knorr and Lohmann (2003) suggest a true South to North direction of the climate change propagation. At this point, one can only state that the latter, observational studies do not contradict the earlier, modeling studies, but do not directly confirm them either.

Many DO models — e.g., Buizert & Schmittner (2015), Dokken et al. (2013), Ganopolski & Rahmstorf (2001), Lohman & Ditlevsen (2018, 2019), Peltier & Vettoretti (2014), Shaffer et al. (2004), Klockmann et al. (2018), Menviel et al. (2014, 2021), and Timmermann et al. (2003) — have not specifically addressed the issue of the interhemispheric signal's direction. To address this issue, Boers et al. (2018) recently developed a simple model to reconstruct the millennial variability in $\delta^{18}O$ of the past 60 kyr b2K, as observed in the high-resolution ice cores from NGRIP in Greenland and West Antarctic Ice Sheet (WAIS) in Antarctica. This simple model, based on the bipolar seesaw mechanism (Stocker and Johnsen, 2003), combines the interactions between ice shelves and sea ice extents, subsurface water temperatures in the North Atlantic Ocean, atmospheric temperature in Greenland, the AMOC strength, and $\delta^{18}O$ in both Greenland and Antarctica. The interplay of the feedbacks involved allowed the authors to reproduce the millennial-scale variability observed in both hemispheres, despite the lack of any time-dependent forcing that would involve orbital parameters.

5. DO events and Bond cycles

The results outlined in the previous section have led us to concentrate on the canonical DOs for which the temperature reconstruction has been proposed based on ^{15}N measurements from the Greenland ice (Guillevic et al., 2014). These estimates indicate that the 21 warming events during the last climate cycle, between 12 ka and 87 ka b2k, had on average a range of 10°C –12°C (Kindler et al., 2014), with each transition lasting on average between 50 yr and 100 yr (Wolff et al., 2010; Rousseau et al., 2017a, b, 2021), as found at least near the top of the Greenland ice sheet at the coring site. Not only does the change in temperature over such a short time imply a drastic reorganization of the atmospheric, and associated marine, circulations (Boers et al., 2018),

but the timing does not correspond to any periodicity of the orbital parameters, neither in the average duration of the events, nor in the average interval between two such events; see Supp. Fig. 2.

The recurrence analysis performed on the high-resolution NGRIP $\delta^{18}O$ record and illustrated in Figs. 4b and 5b suggests looking for other mechanisms that might cause the abrupt changes mentioned previously. As for the $\delta^{18}O$ record analysis in core U1308 displayed in Figs. 2 and 3, the NGRIP study shows a drift topology but with a non-uniform pattern. The RP shows changes in the system's regime of behavior, as identified by transitions detected by analyzing the RR values. The RR analysis of the NGRIP $\delta^{18}O$ values identified seven major transitions. Seven more indicate an RR close to the selected threshold; see Tabs. 1 and 3. Numerous thresholds identified correspond to key dates of the last climate cycle stratigraphy (Bassinot et al., 1994; McManus et al., 1994; Kukla et al., 1997; Lisiecki and Raymo, 2005; Clark et al., 2009); see Tab. 3.

When plotted in Fig. 5c against the variations in global sea level deduced from North Atlantic and Equatorial Pacific $\delta^{18}O$ benthic records by Waelbroeck et al. (2002), the length of the GIs appears to be related to the mean sea level; see Supp. Fig. 3. The long GIs occurred between 120 and 80 ka b2k, and between 59 and 40 ka b2k. During these two intervals, the global sea level exhibited relatively slight variations between about –15 m and –45 m and about –50 m and –75 m, respectively. Conversely, after 80 ka b2K and after 32 ka b2k, GIs were shorter and occurred during the most abrupt drops in sea level of the last climate cycle, from –15 m to –85 m, and from –75 m down to a minimum of about –120 m during the Last Glacial Maximum. The agreement between the results of the recurrence analysis and the NGRIP $\delta^{18}O$ transitions, as well as the link between the length of GIs and the global sea level variations, seems to establish a relation between the variation in GI length and the spatial extent and elevation of the largest continental ice sheets, especially in the Northern Hemisphere, with the latter expanding further inland and out onto the continental shelf during the last climate cycle.

The DO cycles have been grouped together following an overall cooling trend of the GSs and subsequent to a strong DO event (Bond et al., 1992; Alley, 1998; Alley et al., 1999; Clark et al., 2007). This cooling trend ends with a final and coldest GS that coincides with an HE. These groupings have been named Bond cycles (Broecker, 1994; Alley, 1998), and they have been observed mainly in North Atlantic marine records of the last climate cycle with a rough periodicity of 7 kyr (Clark et al., 2007); see Figs. 6 a,b. These Bond cycles, like the DO cycles, have no relationship with the periodicity of the orbital parameters (Supp. Tab. 1), but they are in excellent agreement with the robust 6-7 kyr periodicity of a natural, intrinsic paleoclimate oscillator (Källèn et al., 1979; Ghil and Le Treut, 1981).

This oscillator is based on the countervailing effects of the positive ice-albedo feedback on Earth's radiation balance — with temperatures drops that are enhanced by the increasing extent of sea ice (Budyko, 1969; Sellers, 1969)— and of the negative precipitation-temperature feedback on the mass balance of ice sheets, with temperature increases that contribute to increased accumulation of the ice (Källèn et al., 1979; Miller and De Vernal, 1992; Ghil, 1994; Tziperman and Gildor, 2003). Ghil and Tavantzis (1983) showed that the oscillator's 6-7 kyr periodicity is quite stable over a substantial range of parameter values, and Ghil (1994) noted that this periodicity was predicted by Källén et al. (1979), well before the HEs were discovered by Heinrich (1988). More recently, the HEs' approximate recurrence time was found to be equal roughly to this

periodicity by Clark et al. (2007, and references therein), in spite of the fact that these authors were not aware of its theoretical prediction of M. Ghil and coauthors (Källèn et al., 1979; Ghil and Le Treut, 1981; Ghil, 1994).

The HEs are believed to first occur at about 0.65 Ma, as can be deduced from the U1308 bulk carbonate $\delta^{18}O$ records. The GSs' duration has sometimes been incorrectly linked with the occurrence of an HE, leading to the misinterpretation of HEs as being equivalent to GSs. A detailed study of a subset of GSs has demonstrated that HEs did not last the entire duration of a GS (Guillevic et al., 2014), indicating a much more complex dynamics of the cold stadials themselves than had initially been considered. Such complex climate behavior, by extension, may have prevailed since the first occurrence of HEs in the North Atlantic at about 0.65 Ma. Moreover, Bond and Lotti (1995) demonstrated that although an HE was embedded into the final GS of the Bond cycles, additional IRD events, of lower magnitude than an HE, were also embedded in the previous and intermediary GSs.

Therefore, the previous definition of the Bond cycles given by Lehman (1993), Broecker (1994) and Alley (1998), could be revisited by including the IRD events embedded in every stadial (Figs. 7a,b). Thus Bond cycles should be interpreted as a sequence of DO cycles, which starts with a distinctly warm GI, followed by a cooling trend with increasingly colder GSs that include as many IRD events as the stadials being identified, the latest of which is an HE; see Figs. 6a,b.

The synthetic Greenland $\delta^{18}O$ record reconstructed from the EPICA data over the last 800 ka by applying the bipolar seesaw model (Barker et al., 2011) indicates that DO cycles have occurred at least during this time interval. This synthetic record is, furthermore, well correlated with $\delta^{18}O$ variations observed from Chinese speleothems (Cheng et al., 2016). Hence, the millennial variability associated with the DO cycles is likely to have existed since 0.8 Ma, or even since 0.9 Ma, when the global ice volume strongly increased, as indicated by MIS 22 $\delta^{18}O$ and sea level values. Birner et al. (2016) report millennial variability already during the much older time interval 1235 ka –1220 ka, i.e., MIS41-37, from a marine record on the Iberian Margin. Although detecting variations in planctonic $\delta^{18}O$ that are comparable to the MIS3 DO events in intensity and sawtooth shape, Birner et al. (2016) indicate that "identifying further Bond-like cycles in MIS 38 and 40 is ambiguous. Although the lack of additional cycles might be due to the short duration of glacials in the 41 ka world, the occurrence of Bond-like cycles in the early Pleistocene would not necessarily be expected, owing to their intrinsic relationship to Heinrich events [Bond et al., 1993] that have not been observed in the early Pleistocene [Hodell et al., 2008].", in particular the closing stadial of these cycles does not show a massive IRD discharge, or HE, as described during the last climate cycle.

However, since IRD delivery to the North Atlantic requires ice sheets to reach the ocean, and since the first IRDs are recorded in the North Atlantic at about 1.5 Ma (Hodell and Channell, 2016), one could assume that the start of this type of millennial variability occurred as early as this older threshold. Whether a younger start date of 0.9 Ma, or an older one of 1.5Ma, is posited, these dates show that the Northern Hemisphere ice sheets played a significant role in the onset of millennial and sub-millennial climate variability that prevailed during the Mid and Late Pleistocene.

Ziemen et al. (2019) simulated HEs following the Binge-Purge model of MacAyeal (1993) and reported a two-step mechanism. The first step is a surge phase with enhanced fresh water discharge weakening the deep water formation due to the stratification of the surface water, increased sea ice cover, and leading to reduced North Atlantic sea surface temperature due to a weakened AMOC, reduced evaporation and precipitation. The

second step corresponds to a post-surge phase with a much-lowered elevation of the Laurentide ice sheet that may have lost several hundreds of meters or more during the massive iceberg discharges. During the post-surge phase described by Ziemen et al. (2019), a higher sea level associated with the lower elevation of the ice sheet favors the northern polar jet to move northwards, which leads to more precipitation over Hudson Bay, speeds up the regrowth of the Laurentide ice sheet, and results in the start of a new Bond cycle. A similar mechanism, albeit of lower magnitude, could be considered for the other iceberg discharges occurring during GS, which did not yield HEs. Such a mechanism may apply, with reduced amplitude, to the smaller Eurasian ice sheets that were also involved in the release of icebergs during HEs. The Ziemen et al. (2019) mechanism appears, moreover, to be in agreement with the Mg/Ca data on benthic foraminifera studied by Marcott et al. (2011). These authors found that warming of the subsurface temperature of the high-latitude North Atlantic lead to increased basal melting under ice shelves, accelerated their collapse as suggested by Boers et al. (2018), and thus drove the Hudson Strait Ice Stream of the Laurentide ice sheet to release IRD deposited as HEs (Alvarez-Solas and Ramstein, 2011); see Fig. 7c.

Guillevic et al. (2014) studied ^{17}O excess variations in Greenland ice cores, which characterize changes in the lower-latitude hydrological cycle, and reported that, at least for HE4 and HE5, iceberg delivery to the North Atlantic did not last the whole GS duration. Instead, this delivery occurred about a hundred years after the start of the GS. This short interval seems to correspond to the time during which the subsurface warming of the ocean was linked to an expansion of the sea ice and the ice shelves, as initially mentioned by Marcott et al. (2011) and Boers et al. (2018), and it also corresponds to ”pre-surge” conditions, according to the Ziemen et al. (2019) model, increasing the flow of ice beyond a certain threshold leads to the massive calving of icebergs (surge phase). Furthermore, Guillevic et al. (2014) indicate that the HE4 post-surge started during GS9, hundreds of years prior to the start of the warming corresponding to GI8.

These sequences — starting with a strong GI, followed by intermediary GSs that include IRD events, and ending with a colder GS that includes an HE, see Figs. 7a,b — must have repeated throughout the last climate cycle, most likely so during the glacial interval from 116 ka b2k on Bond and Lotti (1995). In fact, HEs are believed to first occur at about 0.65 Ma, although DO events may have occurred independently since about 0.8 Ma or even 0.9 Ma. It thus appears that the millennial and sub-millennial variability corresponding to the Bond cycles involves variations in size and elevation of the Northern Hemisphere ice sheets that give rise to the iceberg release events into the North Atlantic; see Fig. 7c. This mechanism may have played a key role during the past 0.8 Myr–0.9 Myr, when the Northern Hemisphere ice sheets were at their maximum size and extended out over the continental shelf. This combination of size and contact with the much warmer ocean is likely to have destabilized the ice sheets around the North Atlantic and led to massive IRD events. The appearance of IRD in the North Atlantic Ocean, though, might have occurred as early as 1.5 Ma (Hodell & Channel, 2016), a fact that might suggest the prevalence of the short-periodic variability discussed herein over the last 1.5 Myr.

In any case, a time interval of the most recent 0.8 Myr or 1.5 Myr seems to have witnessed millennial-scale climate variability with an amplitude that exceeded the one due to the direct forcing by the orbital periodicities (Ghil and Childress, 1987; Ghil, 1994; Riechers et al., 2021). This fairly well-agreed-upon fact leads support to the interpretation of the enhanced millennial variability during glacial times as arising from an internal oscillation of the climate system — which could well be consistent with the amended Bond cycle that we have proposed — as well as with the mechanisms proposed by several authors, such as Källèn et al. (1979), Le Treut et al.

(1988), Saltzman (2002) and Crucifix (2012), among others — while Hodell and Channell (2016) only considered it as noise superimposed on the orbital variability deduced from their wavelet analysis of the benthic $\delta^{18}O$ record of U1308. Substantial, nonlinear interactions between internal, oscillatory variability and orbital forcing are actively being explored by Riechers et al.(2021) in this special issue.

6. Concluding remarks

Our quick overview of millennial-scale climate variability over the last 3.2 Myr suggests the following conclusions:

- The key phenomena that characterize this millennial-scale variability are Heinrich events (HEs), Dansgaard-Oeschger (DO) events, and Bond cycles. Abrupt changes are intimately interwoven with these phenomena.
- Present investigations — including both recurrence plot (RP) analysis and Kolmogorov-Smirnov (KS) methodology — point to internal mechanisms being responsible for these millennial-scale events and for the associated abrupt changes. These mechanisms include internal oscillations of the ice sheet–ocean–atmosphere system and episodic calving of ice sheets.
- The Bond cycles are linked to the dynamics of the Northern Hemisphere ice sheets, specifically to variations in their spatial extent and their elevation. The classical Bond cycles end by massive iceberg discharges into the North Atlantic Ocean mainly from the Laurentide ice sheet, but also from the Fennoscandian, Greenland, Iceland and British ice sheets. IRD releases to the North Atlantic have been documented as well during every stadial. Therefore a link with the Northern Hemisphere ice sheets extent appears evident in order to allow iceberg calving into the North Atlantic, whatever the magnitude of the calving event, whether IRD events or HEs. These Bond cycles in their new interpretation illustrate a much more complex millennial variability than initially contemplated, by considering the DO and HE not individually, but linking them into a unified story.
- Millennial-scale variability is observed in proxy records from the very beginning of the last glacial period, and during previous glacial periods, at least since 0.8–0.9 Ma, when HEs first appear in the records. This timing seems to coincide roughly with the MPT that has been associated with a global increase in ice volume on Earth. This coincidence does not exclude the possibility of an even earlier appearance of millennial variability (Birner et al., 2016), given the first appearance of IRD events as early as 1.5 Ma.
- Dynamical interactions between the ocean, the cryosphere with its continental ice sheets and sea ice cover, and the atmosphere are at play in generating the millennial-scale variability during glacials that leads to abrupt climate changes. The specific mechanisms of these interactions, though, are still being elucidated.
- Even so, we have seen that orbital forcing, as postulated by Milankovitch, sets the stage for these internal processes and modulates their period and amplitude.

Orbital-scale and millennial variability appear to interact during the Quaternary, with millennial variability increasing in intensity, as ice sheets grew larger in both area and volume. Thus, abrupt climate changes are undoubtedly related, albeit indirectly, to the astronomical theory of climate.

Author contributions

DDR designed the project and drafted the paper. WB performed the recurrence analyses. All the authors contributed to the writing of the paper. DDR and MG finalized the paper.

Competing interest

The authors declare that they have no conflict of interest. The lead author, as a co-chief editor of Climate of the Past, did not have access to the whole review process.

Acknowledgements

The authors thank the editor, two anonymous reviewers and Linda Hinnov for their handling of the paper and useful comments which greatly benefit the revised version of the original draft. It is a pleasure to acknowledge Laurie Menviel for providing the sea surface maps used in figure 6 and Peter Clark for his comments on the draft of this manuscript. An earlier version of this paper has been presented at the Milankovich symposium held in 2020 to celebrate the centennial of the Milankovitch (1920) book, and DDR sincerely thanks the meeting organizers for inviting DDR to do so. WB, MG and DDR, are funded by the European Union's Horizon 2020 research and innovation programme through the TiPES grant no. 820970. This is LDEO contribution and TiPES contribution (no. x).

Financial support

This research has been supported by the European Union's Horizon 2020 research and innovation programme (TiPES grant no. 820970).

Datasets used

The datasets used include the following:

- Waelbroeck, C.; Labeyrie, L.D.; Michel, E.; Duplessy, J.-C.; McManus, J.F.; Lambeck, K.; Balbon, E.; Labracherie, M. (2010-11-16): NOAA/WDS Paleoclimatology - Sea-level and Deep Water Temperature 430 kyr Reconstructions. NOAA National Centers for Environmental Information. https://www.ncdc.noaa.gov/paleo/study/10496.

- Hodell, D. A.; Channell, J. E. T. (2016): Foraminiferal stable isotopes and physical properties from North Atlantic sediment cores for the past 3.2 million years. PANGAEA, https://doi.org/10.1594/PANGAEA.871937, Supplement to: Hodell, DA; Channell, JET (2016): Mode transitions in Northern Hemisphere glaciation: co-evolution of millennial and orbital variability in Quaternary climate. Climate of the Past, 12(9), 1805-1828, https://doi.org/10.5194/cp-12-1805-2016

- Westerhold, Th. (2020): Cenozoic global reference benthic carbon and oxygen isotope dataset (CENOGRID). PANGAEA, https://doi.org/10.1594/PANGAEA.917503

- Rasmussen, S. O., Bigler, M., Blockley, S. P., Blunier, T., Buchardt, S. L., Clausen, H. B., Cvijanovic, I., Dahl-Jensen, D., Johnsen, S. J., Fischer, H., Gkinis, V., Guillevic, M., Hoek, W. Z., Lowe, J. J., Pedro, J. B., Popp, T., Seierstad, I. K., Steffensen, J. P., Svensson, A. M., Vallelonga, P., Vinther, B. M., Walker, M. J. C., Wheatley, J. J., and Winstrup, M.: A stratigraphic framework for abrupt climatic changes during the Last Glacial period based on three synchronized Greenland ice-core records: refining and extending the INTIMATE event stratigraphy, Quat. Sci. Rev., 106, 14–28,

https://www.iceandclimate.nbi.ku.dk/data/GICC05modelext_GRIP_and_GISP2_and_resampled_data_series_Seierstad_et_al._2014_version_10Dec2014-2.xlsx

- Bond, Gerard C; Heinrich, Hartmut; Broecker, Wallace S; Labeyrie, Laurent D; McManus, Jerry F; Andrews, John T; Huon, Sylvain; Jantschik, Ruediger; Clasen, Silke; Simet, Christine; Tedesco, Kathy; Klas, Mieczyslawa; Bonani, Georges; Ivy, Susan; Obrochta, Stephen P (2012): (Table S3) Abundance of Neogloboquadrina pachyderma (s) in MIS4-2 of DSDP Site 94-609. PANGAEA, https://doi.org/10.1594/PANGAEA.834692, In supplement to: Obrochta, Stephen P; Miyahara, Hiroko; Yokoyama, Yusuke; Crowley, Thomas J (2012): A re-examination of evidence for the North Atlantic "1500-year cycle" at Site 609. Quat. Sci. Rev., 55, 23-33, https://doi.org/10.1016/j.quascirev.2012.08.008

The tables generated by this paper will be submitted to PANGAEA data repository.

References

Adhémar, J.: Révolutions de la mer, déluges périodiques., Carilian-Goeury et V. Dalmont, Paris, 1842.

Agassiz, L.: Glaciers, Moraines, and Erratic Blocks, Edinb. New Philos. J., 24, 364–383, 1838.

Agassiz, L.: Glaciers and the evidence of their having once existed in Scotland, Ireland and England, Proc. Geol. Soc. Lond., III, Part II, 327–332, 1842.

Allen, J. R. M., Brandt, U., Brauer, A., Hubberten, H. W., Huntley, B., Keller, J., Kraml, M., Mackensen, A., Mingram, J., Negendank, J. F. W., Nowaczyk, N. R., Oberhansli, H., Watts, W. A., Wulf, S., and Zolitschka, B.: Rapid environmental changes in southern Europe during the last glacial period, Nature, 400, 740–743, 1999.

Alley, R. B.: Palaeoclimatology - Icing the north Atlantic, Nature, 392, 335-+, https://doi.org/10.1038/32781, 1998.

Alley, R. B., Clark, P. U., Keigwin, L. D., and Webb, R. S.: Making sense of millenial-scale climate change, Mechanisms of global climate change at millenial time scales, 385–394, https://doi.org/10.1029/GM112p0385, 1999.

Alvarez-Solas, J. and Ramstein, G.: On the triggering mechanism of Heinrich events, Proc. Natl. Acad. Sci. U. S. A., 108, E1359–E1360, https://doi.org/10.1073/pnas.1116575108, 2011.

Andrews, J. T. and Voelker, A. H. L.: "Heinrich events" (& sediments): A history of terminology and recommendations for future usage, Quat. Sci. Rev., 187, 31–40, https://doi.org/10.1016/j.quascirev.2018.03.017, 2018.

Bagniewski, W., Ghil, M., Rousseau, D.-D., and American Geopysical Union: Tipping points in the climate system: Automatic detection of abrupt transitions in paleoclimate records, 2020.

Bagniewski, W., Ghil, M., and Rousseau, D. D.: Automatic detection of abrupt transitions in paleoclimate records, Chaos, 31, 113129, https://doi.org/10.1063/5.0062543, 2021.

Barbante, C., Barnola, J. M., Becagli, S., Beer, J., Bigler, M., Boutron, C., Blunier, T., Castellano, E., Cattani, O., Chappellaz, J., Dahl-Jensen, D., Debret, M., Delmonte, B., Dick, D., Falourd, S., Faria, S., Federer, U., Fischer, H., Freitag, J., Frenzel, A., Fritzsche, D., Fundel, F., Gabrielli, P., Gaspari, V., Gersonde, R., Graf, W., Grigoriev, D., Hamann, I., Hansson, M., Hoffmann, G., Hutterli, M. A., Huybrechts, P., Isaksson, E., Johnsen, S., Jouzel, J., Kaczmarska, M., Karlin, T., Kaufmann, P., Kipfstuhl, S., Kohno, M., Lambert, F., Lambrecht, A., Lambrecht, A., Landais, A., Lawer, G., Leuenberger, M., Littot, G., Loulergue, L., Luthi, D., Maggi, V., Marino, F., Masson-Delmotte, V., Meyer, H., Miller, H., Mulvaney, R., Narcisi, B., Oerlemans, J., Oerter, H., Parrenin, F., Petit, J. R., Raisbeck, G., Raynaud, D., Rothlisberger, R., Ruth, U., Rybak, O., Severi, M., Schmitt, J., Schwander, J., Siegenthaler, U., Siggaard-Andersen, M. L., Spahni, R., Steffensen, J. P., Stenni, B., Stocker, T. F., Tison, J. L., Traversi, R., Udisti, R., Valero-Delgado, F., van den Broeke, M. R., van de Wal, R. S. W., Wagenbach, D., Wegner, A., Weiler, K., Wilhelms, F., Winther, J. G., Wolff, E., and Epica Community Members: One-to-one coupling of glacial climate variability in Greenland and Antarctica, Nature, 444, 195–198, https://doi.org/10.1038/nature05301, 2006.

Barker, S., Knorr, G., Edwards, R. L., Parrenin, F., Putnam, A. E., Skinner, L. C., Wolff, E., and Ziegler, M.: 800,000 Years of Abrupt Climate Variability, Science, 334, 347–351, https://doi.org/10.1126/science.1203580, 2011.

Bassinot, F. C., Labeyrie, L. D., Vincent, E., Quidelleur, X., Shackleton, N. J., and Lancelot, Y.: The astronomical theory of climate and the age of the Brunhes-Matuyama magnetic reversal, Earth Planet. Sci. Lett., 126, 91–108, 1994.

Batchelor, C. L., Margold, M., Krapp, M., Murton, D., Dalton, A. S., Gibbard, P. L., Stokes, C. R., Murton, J. B., and Manica, A.: The configuration of Northern Hemisphere ice sheets through the Quaternary, Nat. Commun., 10, https://doi.org/10.1038/s41467-019-11601-2, 2019.

Behre, K. E.: Biostratigraphy of the last glacial period in Europe., Quat. Sci. Rev., 8, 25–44, 1989.

Benn, D. I., Le Hir, G., Bao, H. M., Donnadieu, Y., Dumas, C., Fleming, E. J., Hambrey, M. J., McMillan, E. A., Petronis, M. S., Ramstein, G., Stevenson, C. T. E., Wynn, P. M., and Fairchild, I. J.: Orbitally forced ice sheet fluctuations during the Marinoan Snowball Earth glaciation, Nat. Geosci., 8, 704–707, https://doi.org/10.1038/ngeo2502, 2015.

Berends, C. J., de Boer, B., and van de Wal, R. S. W.: Reconstructing the evolution of ice sheets, sea level, and atmospheric CO2 during the past 3.6 million years, Clim. Past, 17, 361–377, https://doi.org/10.5194/cp-17-361-2021, 2021.

Berger, A. L.: Support for astronomical theory of climatic change, Nature, 269, 44–45, https://doi.org/10.1038/269044a0, 1977.

Berger, A. L.: Long-term variations of caloric insolation resulting from the Earth's orbital elements., Quat. Res., 9, 139–167, 1978.

Birner, B., Hodell, D. A., Tzedakis, P. C., and Skinner, L. C.: Similar millennial climate variability on the Iberian margin during two early Pleistocene glacials and MIS 3, Paleoceanography, 31, 203–217, https://doi.org/10.1002/2015pa002868, 2016.

Blunier, T. and Brook, E. J.: Timing of millennial-scale climate change in Antarctica and Greenland during the last glacial period, Science, 291, 109–112, https://doi.org/10.1126/science.291.5501.109, 2001.

Boch, R., Cheng, H., Spotl, C., Edwards, R. L., Wang, X., and Hauselmann, P.: NALPS: a precisely dated European climate record 120-60 ka, Clim. Past, 7, 1247–1259, https://doi.org/10.5194/cp-7-1247-2011, 2011.

Boers, N.: Early-warning signals for Dansgaard-Oeschger events in a high-resolution ice core record, Nat. Commun., 9, https://doi.org/10.1038/s41467-018-04881-7, 2018.

Boers, N., Ghil, M., and Rousseau, D. D.: Ocean circulation, ice shelf, and sea ice interactions explain Dansgaard-Oeschger cycles, Proc. Natl. Acad. Sci. U. S. A., 115, E11005–E11014, https://doi.org/10.1073/pnas.1802573115, 2018.

Bond, G., Heinrich, H., Broecker, W., Labeyrie, L., McManus, J., Andrews, J., Huon, S., Jantschik, R., Clasen, S., Simet, C., Tedesco, K., Klas, M., Bonani, G., and Ivy, S.: Evidence for massive discharges of icebergs into the North Atlantic Ocean during the last glacial period., Nature, 360, 245–249, 1992.

Bond, G., Broecker, W., Johnsen, S., McManus, J., Labeyrie, L., Jouzel, J., and Bonani, G.: Correlations between climate records from North Atlantic sediments and Greenland ice., Nature, 365, 143–147, 1993.

Bond, G. C. and Lotti, R.: Iceberg discharges into the North Atlantic on millennial time scales during the last glaciation., Science, 267, 1005–1010, 1995.

Broecker, W. S.: Massive iceberg discharges as triggers for global climate change., Nature, 372, 421–424, 1994.

Broecker, W. S.: Abrupt climate change: causal constraints provided by the paleoclimate record, Earth-Sci. Rev., 51, 137–154, 2000.

Broecker, W. S. and Denton, G.: The role of ocean-atmosphere reorganizations in glacial cycles., Geochim Cosmochim Acta, 53, 2465–2501, 1989.

Broecker, W. S. and van Donk, J.: Insolation changes, ice volumes, and 0-18 record in deep-sea cores, Rev. Geophys. Space Phys., 8, 169–198, https://doi.org/10.1029/RG008i001p00169, 1970.

Broecker, W. S., Andree, M., Bonani, G., Wolfi, W., Oeschger, H., and Klas, M.: Can the Greenland climatic jumps be identified in records from ocean and land?, Quat. Res., 30, 1–6, 1988.

Budyko, M. I.: Effect of solar radiation variations on climate of Earth, Tellus, 21, 611-, https://doi.org/10.3402/tellusa.v21i5.10109, 1969.

Buizert, C. and Schmittner, A.: Southern Ocean control of glacial AMOC stability and Dansgaard-Oeschger interstadial duration, Paleoceanography, 30, 1595–1612, https://doi.org/10.1002/2015pa002795, 2015.

Buizert, C., Adrian, B., Ahn, J., Albert, M., Alley, R. B., Baggenstos, D., Bauska, T. K., Bay, R. C., Bencivengo, B. B., Bentley, C. R., Brook, E. J., Chellman, N. J., Clow, G. D., Cole-Dai, J., Conway, H., Cravens, E., Cuffey, K. M., Dunbar, N. W., Edwards, J. S., Fegyveresi, J. M., Ferris, D. G., Fitzpatrick, J. J., Fudge, T. J., Gibson, C. J., Gkinis, V., Goetz, J. J., Gregory, S., Hargreaves, G. M., Iverson, N., Johnson, J. A., Jones, T. R., Kalk, M. L., Kippenhan, M. J., Koffman, B. G., Kreutz, K., Kuhl, T. W., Lebar, D. A., Lee, J. E., Marcott, S. A., Markle, B. R., Maselli, O. J., McConnell, J. R., McGwire, K. C., Mitchell, L. E., Mortensen, N. B., Neff, P. D., Nishiizumi, K., Nunn, R. M., Orsi, A. J., Pasteris, D. R., Pedro, J. B., Pettit, E. C., Price, P. B., Priscu, J. C., Rhodes, R. H., Rosen, J. L., Schauer, A. J., Schoenemann, S. W., Sendelbach, P. J., Severinghaus, J. P., Shturmakov, A. J., Sigl, M., Slawny, K. R., Souney, J. M., Sowers, T. A., Spencer, M. K., Steig, E. J., Taylor, K. C., Twickler, M. S., Vaughn, B. H., Voigt, D. E., Waddington, E. D., Welten, K. C., Wendricks, A. W., White, J. W. C., Winstrup, M., Wong, G. J., Woodruff, T. E., and Wais Divide Project Members: Precise interpolar phasing of abrupt climate change during the last ice age, Nature, 520, 661-U169, https://doi.org/10.1038/nature14401, 2015a.

Buizert, C., Adrian, B., Ahn, J., Albert, M., Alley, R. B., Baggenstos, D., Bauska, T. K., Bay, R. C., Bencivengo, B. B., Bentley, C. R., Brook, E. J., Chellman, N. J., Clow, G. D., Cole-Dai, J., Conway, H., Cravens, E., Cuffey, K. M., Dunbar, N. W., Edwards, J. S., Fegyveresi, J. M., Ferris, D. G., Fitzpatrick, J. J., Fudge, T. J., Gibson, C. J., Gkinis, V., Goetz, J. J., Gregory, S., Hargreaves, G. M., Iverson, N., Johnson, J. A., Jones, T. R., Kalk, M. L., Kippenhan, M. J., Koffman, B. G., Kreutz, K., Kuhl, T. W., Lebar, D. A., Lee, J. E., Marcott, S. A., Markle, B. R., Maselli, O. J., McConnell, J. R., McGwire, K. C., Mitchell, L. E., Mortensen, N. B., Neff, P. D., Nishiizumi, K., Nunn, R. M., Orsi, A. J., Pasteris, D. R., Pedro, J. B., Pettit, E. C., Price, P. B., Priscu, J. C., Rhodes, R. H., Rosen, J. L., Schauer, A. J., Schoenemann, S. W., Sendelbach, P. J., Severinghaus, J. P., Shturmakov, A. J., Sigl, M., Slawny, K. R., Souney, J. M., Sowers, T. A., Spencer, M. K., Steig, E. J., Taylor, K. C., Twickler, M. S., Vaughn, B. H., Voigt, D. E., Waddington, E. D., Welten, K. C., Wendricks, A. W., White, J. W. C., Winstrup, M., Wong, G. J., Woodruff, T. E., and Wais Divide Project Members: Precise interpolar phasing of abrupt climate change during the last ice age, Nature, 520, 661-U169, https://doi.org/10.1038/nature14401, 2015b.

Buizert, C., Cuffey, K. M., Severinghaus, J. P., Baggenstos, D., Fudge, T. J., Steig, E. J., Markle, B. R., Winstrup, M., Rhodes, R. H., Brook, E. J., Sowers, T. A., Clow, G. D., Cheng, H., Edwards, R. L., Sigl, M.,

McConnell, J. R., and Taylor, K. C.: The WAIS Divide deep ice core WD2014 chronology - Part 1: Methane synchronization (68-31 kaBP) and the gas age-ice age difference, Clim. Past, 11, 153–173, https://doi.org/10.5194/cp-11-153-2015, 2015c.

Chappell, J. and Shackleton, N. J.: Oxygen isotopes and sea-level, Nature, 324, 137–140, https://doi.org/10.1038/324137a0, 1986.

Chapront, J., Bretagnon, P., and Mehl, M.: Un formulaire pour le calcul des perturbations d'ordres élevés dans les problèmes planétaires, Celest. Mech., 11, 379–399, https://doi.org/10.1007/BF01228813, 1975.

Cheng, H., Edwards, R. L., Sinha, A., Spotl, C., Yi, L., Chen, S. T., Kelly, M., Kathayat, G., Wang, X. F., Li, X. L., Kong, X. G., Wang, Y. J., Ning, Y. F., and Zhang, H. W.: The Asian monsoon over the past 640,000 years and ice age terminations, Nature, 534, 640–646, https://doi.org/10.1038/nature18591, 2016.

Clark, P. U. and Pollard, D.: Origin of the middle Pleistocene transition by ice sheet erosion of regolith, Paleoceanography, 13, 1–9, 1998.

Clark, P. U., Alley, R. B., and Pollard, D.: Climatology - Northern hemisphere ice-sheet influences on global climate change, Science, 286, 1104–1111, https://doi.org/10.1126/science.286.5442.1104, 1999.

Clark, P. U., Archer, D., Pollard, D., Blum, J. D., Rial, J. A., Brovkin, V., Mix, A. C., Pisias, N. G., and Roy, M.: The middle Pleistocene transition: characteristics. mechanisms, and implications for long-term changes in atmospheric PCO2, Quat. Sci. Rev., 25, 3150–3184, https://doi.org/10.1016/j.quascirev.2006.07.008, 2006.

Clark, P. U., Hostetler, S. W., Pisias, N. G., Schmittner, A., and Meissner, K. J.: Mechanisms for an ~7-kyr climate and sea-level oscillation during marine isotope stage 3, Geophys. Monogr. Ser., 173, 209_246, 2007.

Clark, P. U., Dyke, A. S., Shakun, J. D., Carlson, A. E., Clark, J., Wohlfarth, B., Mitrovica, J. X., Hostetler, S. W., and McCabe, A. M.: The Last Glacial Maximum, Science, 325, 710–714, https://doi.org/10.1126/science.1172873, 2009.

Clark, P. U., Shakun, J., Rosenthal, Y., Köhler, P., Schrag, D., Pollard, D., Liu, Z., Bartlein, P., and EGU: Requiem for the Regolith Hypothesis: Sea-Level and Temperature Reconstructions Provide a New Template for the Middle Pleistocene Transition, 2021.

Croll, J.: Climate and Time, D. Appletown and Company, NY, 1890.

Crucifix, M.: Oscillators and relaxation phenomena in Pleistocene climate theory, Philos. Trans. R. Soc. -Math. Phys. Eng. Sci., 370, 1140–1165, https://doi.org/10.1098/rsta.2011.0315, 2012.

Dansgaard, W., Johnsen, S. J., Moller, J., and Langway, C. C.: One thousand centuries of climatic record from Camp Century on the Greenland ice sheet., Science, 166, 377–381, 1969.

Dansgaard, W., Clausen, H. B., Gundestrup, N., Hammer, C. U. J., ohnsen, S. F., Kristinsdottir, P. M., and Reeh, N.: A new Greenland deep ice core., Science, 218, 1273–1277, 1982.

Dansgaard, W., Johnsen, S. J., Clausen, H. B., Dahi-Jensen, D., Gundestrup, N. S., Hammer, C. U., Hvidberg, C. S., Steffensen, J. P., Sveinbjöprnsdottir, A. E., Jouzel, J., and Bond, G.: Evidence for general instability of past climate from a 250-kyr ice-core record., Nature, 364, 218-220., 1993.

Dokken, T. M., Nisancioglu, K. H., Li, C., Battisti, D. S., and Kissel, C.: Dansgaard-Oeschger cycles: Interactions between ocean and sea ice intrinsic to the Nordic seas, Paleoceanography, 28, 491–502, https://doi.org/10.1002/palo.20042, 2013.

Drury, A. J., Liebrand, D., Westerhold, T., Beddow, H. M., Hodell, D. A., Rohlfs, N., Wikens, R. H., Lyle, M., Bell, D. B., Kroon, D., Pälike, H., and Lourens, L. J.: Climate, cryosphere and carbon cycle controls on Southern Atlantic orbital-scale carbonate deposition since the Oligocene (30-0 Ma), Clim. Past, pre-print, https://doi.org/10.5194/cp-2020-108, 2020.

Eckmann, J. P., Kamphorst, S. O., and Ruelle, D.: Recurrence plots of dynamical systems, Europhys. Lett., 4, 973–977, https://doi.org/10.1209/0295-5075/4/9/004, 1987.

Efron, B.: nonparametric estimates of standard error - The Jackknife, the bootstrap and other methods, Biometrika, 68, 589–599, https://doi.org/10.2307/2335441, 1981.

Efron, B. and Tibshirani, R.: Bootstrap methods for standard errors, confidence intervals, and other measures of statistical accuracy, Stat. Sci., 1, 54–75, https://doi.org/10.1214/ss/1177013815, 1986.

Elderfield, H., Ferretti, P., Greaves, M., Crowhurst, S., McCave, I. N., Hodell, D., and Piotrowski, A. M.: Evolution of Ocean Temperature and Ice Volume Through the Mid-Pleistocene Climate Transition, Science, 337, 704–709, https://doi.org/10.1126/science.1221294, 2012.

Emiliani, C.: Pleistocene temperatures, J. Geol., 63, 538–578, 1955.

Fischer, H., Schuepbach, S., Gfeller, G., Bigler, M., Roethlisberger, R., Erhardt, T., Stocker, T. F., Mulvaney, R., and Wolff, E.: Millennial changes in North American wildfire and soil activity over the last glacial cycle, Nat. Geosci., 8, 723–728, https://doi.org/10.1038/ngeo2495, 2015.

Fleitmann, D., Cheng, H., Badertscher, S., Edwards, R. L., Mudelsee, M., Goektuerk, O. M., Fankhauser, A., Pickering, R., Raible, C. C., Matter, A., Kramers, J., and Tuysuz, O.: Timing and climatic impact of Greenland interstadials recorded in stalagmites from northern Turkey, Geophys. Res. Lett., 36, https://doi.org/10.1029/2009gl040050, 2009.

Fletcher, W. J., Goni, M. F. S., Allen, J. R. M., Cheddadi, R., Combourieu-Nebout, N., Huntley, B., Lawson, I., Londeix, L., Magri, D., Margari, V., Mueller, U. C., Naughton, F., Novenko, E., Roucoux, K., and Tzedakis, P. C.: Millennial-scale variability during the last glacial in vegetation records from Europe, Quat. Sci. Rev., 29, 2839–2864, https://doi.org/10.1016/j.quascirev.2009.11.015, 2010.

Flint, R. F.: Glacial and Quaternary geology, 1971.

Ganopolski, A. and Rahmstorf, S.: Rapid changes of glacial climate simulated in a coupled climate model, Nature, 409, 153–158, 2001.

Genty, D., Blamart, D., Ouahdi, R., Gilmour, M., Baker, A., Jouzel, J., and Van-Exter, S.: Precise dating of Dansgaard-Oeschger climate oscillations in western Europe from stalagmite data, Nature, 421, 833–837, 2003.

Ghil, M.: Cryothermodynamics - The chaotic dynamics of paleoclimate, Phys. -Nonlinear Phenom., 77, 130–159, https://doi.org/10.1016/0167-2789(94)90131-7, 1994.

Ghil, M. and Childress, S.: Topics in Geophysical Fluid Dynamics: Atmospheric Dynamics, Dynamo Theory and Climate Dynamics, Springer-Verlag, New-York, 485 pp., 1987.

Ghil, M. and Le Treut, H.: A climate model with cryodynamics and geodynamics, J. Geophys. Res.-Oceans, 86, 5262–5270, https://doi.org/10.1029/JC086iC06p05262, 1981.

Ghil, M. and Tavantzis, J.: Global Hopf-bifurcation in a simple climate model, Siam J. Appl. Math., 43, 1019–1041, https://doi.org/10.1137/0143067, 1983.

Guillevic, M., Bazin, L., Landais, A., Stowasser, C., Masson-Delmotte, V., Blunier, T., Eynaud, F., Falourd, S., Michel, E., Minster, B., Popp, T., Prie, F., and Vinther, M.: Evidence for a three-phase sequence during Heinrich Stadial 4 using a multiproxy approach based on Greenland ice core records, Clim. Past, 10, 2115–2133, https://doi.org/10.5194/cp-10-2115-2014, 2014.

Hays, J. D., Imbrie, J., and Shackleton, N. J.: Variations in the Earth's Orbit: Pacemaker of the Ice Ages., Science, 194, 1121–1132, 1976.

Heinrich, H.: Origin and Consequences of Cyclic Ice Rafting in the Northeast Atlantic Ocean during the Past 130,000 years, Quat. Res., 29, 142–152, 1988.

Hemming, S. R.: Heinrich events: Massive late Pleistocene detritus layers of the North Atlantic and their global climate imprint., Rev. Geophys., 42, doi:10.1029/2003RG000128, 2004.

Henry, L. G., McManus, J. F., Curry, W. B., Roberts, N. L., Piotrowski, A. M., and Keigwin, L. D.: North Atlantic ocean circulation and abrupt climate change during the last glaciation, Science, 353, 470–474, https://doi.org/10.1126/science.aaf5529, 2016.

Hinnov, L. A.: Cyclostratigraphy and its revolutionizing applications in the earth and planetary sciences, Geol. Soc. Am. Bull., 125, 1703–1734, https://doi.org/10.1130/b30934.1, 2013.

Hinnov, L. A.: Chapter One - Cyclostratigraphy and Astrochronology in 2018, in: Stratigraphy & Timescales, vol. 3, edited by: Montenari, M., Academic Press, 1–80, https://doi.org/10.1016/bs.sats.2018.08.004, 2018.

Hinnov, L. A., Schulz, M., and Yiou, P.: Interhemispheric space-time attributes of the Dansgaard-Oeschger oscillations between 100 and 0ka, Quat. Sci. Rev., 21, 1213–1228, 2002.

Hodell, D. A. and Channell, J. E. T.: Mode transitions in Northern Hemisphere glaciation: co-evolution of millennial and orbital variability in Quaternary climate, Clim. Past, 12, 1805–1828, https://doi.org/10.5194/cp-12-1805-2016, 2016.

Hodell, D. A., Channell, J. E. T., Curtis, J. H., Romero, O. E., and Roehl, U.: Onset of "Hudson Strait" Heinrich events in the eastern North Atlantic at the end of the middle Pleistocene transition (similar to 640 ka)?, Paleoceanography, 23, https://doi.org/10.1029/2008pa001591, 2008.

Hoffman, P. F., Abbot, D. S., Ashkenazy, Y., Benn, D. I., Brocks, J. J., Cohen, P. A., Cox, G. M., Creveling, J. R., Donnadieu, Y., Erwin, D. H., Fairchild, I. J., Ferreira, D., Goodman, J. C., Halverson, G. P., Jansen, M. F., Le Hir, G., Love, G. D., Macdonald, F. A., Maloof, A. C., Partin, C. A., Ramstein, G., Rose, B. E. J., Rose, C. V., Sadler, P. M., Tziperman, E., Voigt, A., and Warren, S. G.: Snowball Earth climate dynamics and Cryogenian geology-geobiology, Sci. Adv., 3, https://doi.org/10.1126/sciadv.1600983, 2017.

Imbrie, J. P. and Imbrie, K.: Ice Ages solving the mystery, Harvard University Press, 224 pp., 1979.

Jakob, K. A., Wilson, P. A., Pross, J., Ezard, T. H. G., Fiebig, J., Repschlager, J., and Friedrich, O.: A new sea-level record for the Neogene/Quaternary boundary reveals transition to a more stable East Antarctic Ice Sheet, Proc. Natl. Acad. Sci. U. S. A., 117, 30980–30987, https://doi.org/10.1073/pnas.2004209117, 2020.

Johnsen, S. J., Dansgaard, W., Clausen, H. B., and Langway, C. C.: Oxygen isotope profiles through the Antartic and Greenland ice sheets., Nature, 235, 429–434, 1972.

Johnsen, S. J., Dahl-Jensen, D., Gundestrup, N., Steffensen, J. P., Clausen, H. B., Miller, H., Masson-Delmotte, V., Sveinbjörnsdottir, A. E., and White, J.: Oxygen isotope and palaeotemperature records from six Greenland ice-core stations: Camp Century, Dye-3, GRIP, GISP2, Renland and NorthGRIP, J. Quat. Sci., 16, 299–307, 2001.

Källèn E., Crafoord, C., and Ghil, M.: Free oscillations in a climate model with ice-sheet dynamics, J. Atmospheric Sci., 36, 2292–2303, https://doi.org/10.1175/1520-0469(1979)036<2292:foiacm>2.0.co;2, 1979.

Kent, D. V., Olsen, P. E., and Muttoni, G.: Astrochronostratigraphic polarity time scale (APTS) for the Late Triassic and Early Jurassic from continental sediments and correlation with standard marine stages, Earth-Sci. Rev., 166, 153–180, https://doi.org/10.1016/j.earscirev.2016.12.014, 2017.

Kent, D. V., Olsen, P. E., Rasmussen, C., Lepre, C., Mundil, R., Irmis, R. B., Gehrels, G. E., Giesler, D., Geissman, J. W., and Parker, W. G.: Empirical evidence for stability of the 405-kiloyear Jupiter-Venus eccentricity cycle over hundreds of millions of years, Proc. Natl. Acad. Sci. U. S. A., 115, 6153–6158, https://doi.org/10.1073/pnas.1800891115, 2018.

Kindler, P., Guillevic, M., Baumgartner, M., Schwander, J., Landais, A., and Leuenberger, M.: Temperature reconstruction from 10 to 120 kyr b2k from the NGRIP ice core, Clim. Past, 10, 887–902, https://doi.org/10.5194/cp-10-887-2014, 2014.

Klockmann, M., Mikolajewicz, U., and Marotzke, J.: Two AMOC States in Response to Decreasing Greenhouse Gas Concentrations in the Coupled Climate Model MPI-ESM, J. Clim., 31, 7969–7984, https://doi.org/10.1175/jcli-d-17-0859.1, 2018.

Knudsen, M. F., Norgaard, J., Grischott, R., Kober, F., Egholm, D. L., Hansen, T. M., and Jansen, J. D.: New cosmogenic nuclide burial-dating model indicates onset of major glaciations in the Alps during Middle Pleistocene Transition, Earth Planet. Sci. Lett., 549, https://doi.org/10.1016/j.epsl.2020.116491, 2020.

Kukla, G., McManus, J. F., Rousseau, D. D., and Chuine, I.: How long and how stable was the last interglacial?, Quat. Sci. Rev., 16, 605–612, 1997.

Laskar, J., Fienga, A., Gastineau, M., and Manche, H.: La2010: a new orbital solution for the long-term motion of the Earth, Astron. Astrophys., 532, https://doi.org/10.1051/0004-6361/201116836, 2011.

Le Treut, H., Portes, J., Jouzel, J., and Ghil, M.: Isotopic modeling of climatic oscillations - Implications for a comparative-study of marine and ice core records, J. Geophys. Res.-Atmospheres, 93, 9365–9383, https://doi.org/10.1029/JD093iD08p09365, 1988.

Le Verrier, U. J.-J.: Théorie et Tables du Mouvement Apparent du Soleil, Ann. Obs. Impérial Paris, 1–64, 1858.

Lehman, S.: Ice sheets, wayward winds and sea change, Nature, 365, 108–110, 1993.

Liebrand, D., Lourens, L. J., Hodell, D. A., de Boer, B., van de Wal, R. S. W., and Paelike, H.: Antarctic ice sheet and oceanographic response to eccentricity forcing during the early Miocene, Clim. Past, 7, 869–880, https://doi.org/10.5194/cp-7-869-2011, 2011.

Lisiecki, L. E. and Raymo, M. E.: A Pliocene-Pleistocene stack of 57 globally distributed benthic delta O-18 records, Paleoceanography, 20, PA1003, doi:10.1029/2004PA001071, 2005.

Lohmann, G., Butzin, M., Eissner, N., Shi, X., and Stepanek, C.: Abrupt Climate and Weather Changes Across Time Scales, Paleoceanogr. Paleoclimatology, 35, https://doi.org/10.1029/2019PA003782, 2020.

Lohmann, J. and Ditlevsen, P. D.: Random and externally controlled occurrences of Dansgaard-Oeschger events, Clim. Past, 14, 609–617, https://doi.org/10.5194/cp-14-609-2018, 2018.

Lohmann, J. and Ditlevsen, P. D.: Objective extraction and analysis of statistical features of Dansgaard-Oeschger events, Clim. Past, 15, 1771–1792, https://doi.org/10.5194/cp-15-1771-2019, 2019.

MacAyeal, D. R.: Binge/purge oscillations of the Laurentide ice sheet as a cause of the North Atlantic Heinrich events, Paleoceanography, 8, 775–784, https://doi.org/10.1029/93pa02200, 1993.

Marcott, S. A., Clark, P. U., Padman, L., Klinkhammer, G. P., Springer, S. R., Liu, Z. Y., Otto-Bliesner, B. L., Carlson, A. E., Ungerer, A., Padman, J., He, F., Cheng, J., and Schmittner, A.: Ice-shelf collapse from subsurface warming as a trigger for Heinrich events, Proc. Natl. Acad. Sci. U. S. A., 108, 13415–13419, https://doi.org/10.1073/pnas.1104772108, 2011.

Marwan, N., Carmen Romano, M., Thiel, M., and Kurths, J.: Recurrence plots for the analysis of complex systems, Phys. Rep., 438, 237–329, https://doi.org/10.1016/j.physrep.2006.11.001, 2007.

Marwan, N., Schinkel, S., and Kurths, J.: Recurrence plots 25 years later - Gaining confidence in dynamical transitions, EPL, 101, https://doi.org/10.1209/0295-5075/101/20007, 2013.

McManus, J. F., Bond, G. C., Broecker, W. S., Johnsen, S., Labeyrie, L., and Higgins, S.: High-resolution climate records from the North Atlantic during the last interglacial., Nature, 371, 326–329, 1994.

McManus, J. F., Oppo, D. W., and Cullen, J. L.: A 0,5-million-year record of millennial-scale climate variability in the North Atlantic, Science, 283, 971–975, 1999.

McManus, J. F., Francois, R., Gherardi, J. M., Keigwin, L. D., and Brown-Leger, S.: Collapse and rapid resumption of Atlantic meridional circulation linked to deglacial climate changes, Nature, 428, 834–837, https://doi.org/10.1038/nature02494, 2004.

Menviel, L., Timmermann, A., Friedrich, T., and England, M. H.: Hindcasting the continuum of Dansgaard-Oeschger variability: mechanisms, patterns and timing, Clim. Past, 10, 63–77, https://doi.org/10.5194/cp-10-63-2014, 2014.

Menviel, L., Skinner, L. C., Tarasov, L., and Tzedakis, P. C.: An ice-climate oscillatory framework for Dansgaard-Oeschger cycles, Narure Rev. Earth Environ., 1, 677–693, https://doi.org/10.1038/s43017-020-00106-y, 2021.

Meyers, S. R. and Malinverno, A.: Proterozoic Milankovitch cycles and the history of the solar system, Proc. Natl. Acad. Sci. U. S. A., 115, 6363–6368, https://doi.org/10.1073/pnas.1717689115, 2018.

Milankovic, M.: Théorie mathématique des Phénomènes thermiques produits par la radiation solaire, edited by: Académie Yougoslave des Sciences et des Arts de Zagreb, Gauthier Villars, Paris, 1920.

Milankovic, M.: Kanon der Erdbestrahlung und seine Anwendung auf das Eiszeitenproblem, Royal Serbian Sciences, Belgrade, 633p pp., 1941.

Miller, G. H. and De Vernal, A.: Will greenhouse warming lead to Northern-Hemisphere ice-sheet growth, Nature, 355, 244–246, https://doi.org/10.1038/355244a0, 1992.

Miller, K. G., Mountain, G. S., Wright, J. D., and Browning, J. V.: A 180-Million-Year Record of Sea Level and Ice Volume Variations from Continental Margin and Deep-Sea Isotopic Records, Oceanography, 24, 40–53, https://doi.org/10.5670/oceanog.2011.26, 2011.

Müller, U. C., Pross, J., and Bibus, E.: Vegetation response to rapid climate change in Central Europe during the past 140,000 yr based on evidence from the Füramoos pollen record, Quat. Res., 59, 235–245, 2003.

Muttoni, G., Carcano, C., Garzanti, E., Ghielmi, M., Piccin, A., Pini, R., Rogledi, S., and Sciunnach, D.: Onset of major Pleistocene glaciations in the Alps, Geology, 31, 989–992, https://doi.org/10.1130/g19445.1, 2003.

Naafs, B. D. A., Hefter, J., and Stein, R.: Millennial-scale ice rafting events and Hudson Strait Heinrich(-like) Events during the late Pliocene and Pleistocene: a review, Quat. Sci. Rev., 80, 1–28, https://doi.org/10.1016/j.quascirev.2013.08.014, 2013.

Obrochta, S. P., Crowley, T. J., Channell, J. E. T., Hodell, D. A., Baker, P. A., Seki, A., and Yokoyama, Y.: Climate variability and ice-sheet dynamics during the last three glaciations, Earth Planet. Sci. Lett., 406, 198–212, https://doi.org/10.1016/j.epsl.2014.09.004, 2014.

Olsen, P. E., Laskar, J., Kent, D. V., Kinney, S. T., Reynolds, D. J., Sha, J. G., and Whiteside, J. H.: Mapping Solar System chaos with the Geological Orrery, Proc. Natl. Acad. Sci. U. S. A., 116, 10664–10673, https://doi.org/10.1073/pnas.1813901116, 2019.

Peltier, W. R. and Vettoretti, G.: Dansgaard-Oeschger oscillations predicted in a comprehensive model of glacial climate: A "kicked" salt oscillator in the Atlantic, Geophys. Res. Lett., 41, 7306–7313, https://doi.org/10.1002/2014gl061413, 2014.

Penck, A. and Brückner, E.: Die Alpen im Eiszeitalter, CHR. Herm. Tauchnitz, Leipzig, 1190 p. pp., 1909.

Pilgrim, L. J. H.: Versuch einer rechnerischen Behandlung des Eiszeitproblems, Gutenberg, 1904.

Pisias, N. G. and Moore, T. C.: The evolution of Pleistocene climate: A time-series approach, Earth Planet. Sci. Lett., 52, 450–458, https://doi.org/10.1016/0012-821x(81)90197-7, 1981.

Rahmstorf, S.: Ocean circulation and climate during the past 120,000 years, Nature, 419, 207–214, 2002.

Railsback, L. B., Gibbard, P. L., Head, M. J., Voarintsoa, N. R. G., and Toucanne, S.: An optimized scheme of lettered marine isotope substages for the last 1.0 million years, and the climatostratigraphic nature of isotope stages and substages, Quat. Sci. Rev., 111, 94–106, https://doi.org/10.1016/j.quascirev.2015.01.012, 2015.

Rasmussen, S. O., Bigler, M., Blockley, S. P., Blunier, T., Buchardt, S. L., Clausen, H. B., Cvijanovic, I., Dahl-Jensen, D., Johnsen, S. J., Fischer, H., Gkinis, V., Guillevic, M., Hoek, W. Z., Lowe, J. J., Pedro, J. B., Popp, T., Seierstad, I. K., Steffensen, J. P., Svensson, A. M., Vallelonga, P., Vinther, B. M., Walker, M. J. C., Wheatley, J. J., and Winstrup, M.: A stratigraphic framework for abrupt climatic changes during the Last Glacial period based on three synchronized Greenland ice-core records: refining and extending the INTIMATE event stratigraphy, Quat. Sci. Rev., 106, 14–28, https://doi.org/10.1016/j.quascirev.2014.09.007, 2014.

Riechers, K., Mitsui, T., Boers, N., and Ghil, Michael: Orbital Insolation Variations, Intrinsic Climate Variability, and Quaternary Glaciations, Clim. Past Discuss., [preprint], https://doi.org/10.5194/cp-2021-136, in review, 2021.

Rousseau, D. D., Svensson, A., Bigler, M., Sima, A., Steffensen, J. P., and Boers, N.: Eurasian contribution to the last glacial dust cycle: how are loess sequences built?, Clim. Past, 13, https://doi.org/10.5194/cp-13-1181-2017, 2017a.

Rousseau, D. D., Boers, N., Sima, A., Svensson, A., Bigler, M., Lagroix, F., Taylor, S., and Antoine, P.: (MIS3 & 2) millennial oscillations in Greenland dust and Eurasian aeolian records - A paleosol perspective, Quat. Sci. Rev., 169, 99–113, https://doi.org/10.1016/j.quascirev.2017.05.020, 2017b.

Rousseau, D.-D., Antoine, P., and Sun, Y.: How dusty was the last glacial maximum over Europe?, Quat. Sci. Rev., 254, 6775–6775, 2021.

Ruddiman, W. F.: Late Quaternary deposition of ice) rafted sand in subpolar North-Atlantic (Lat 40-degrees to 65-degrees-N), Geol. Soc. Am. Bull., 88, 1813–1827, https://doi.org/10.1130/0016-7606(1977)88<1813:lqdois>2.0.co;2, 1977.

Ruddiman, W. F., Raymo, M., Martinson, D. G., Clement, B. M., and Backman, J.: Pleistocene evolution : Northern Hemisphere ice sheets and North Atlantic Ocean., Paleoceanography, 4, 353–412, 1989.

Saltzman, B.: Dynamical Paleoclimatology, Academic Press, San Diego, 354 pp., 2002.

Sanchez-Goni, M. F., Turon, J. L., Eynaud, F., and Gendreau, S.: European climatic response to millennial-scale changes in the atmosphere-ocean system during the last glacial period, Quat. Res., 54, 394–403, 2000.

Sanchez-Goni, M. F., Cacho, I., Turon, J. L., Guiot, J., Sierro, F. J., Peypouquet, J. P., Grimalt, J. O., and Shackleton, N. J.: Synchroneity between marine and terrestrial responses to millennial scale climatic variability during the last glacial period in the Mediterranean region, Clim. Dyn., 19, 95–105, https://doi.org/10.1007/s00382-001-0212-x, 2002.

Sarnthein, M., Stattegger, K., Dreger, D., Erlenkeuser, H., Grootes, P., Haupt, B. J., Jung, S., Kiefer, T., Kuhnt, W., Pflaumann, U., Schafer-Neth, C., Schulz, H., Schulz, M., Seidov, D., Simstich, J., van Kreveld, S., Vogelsang, E., Volker, A., and Weinelt, M.: Fundamental modes and abrupt changes in north Atlantic circulation and climate over the last 60 ky - Concepts, reconstruction and numerical modeling, North. N. Atl. Chang. Environ., 365–410, 2001.

Schulz, M.: On the 1470-year pacing of Dansgaard-Oeschger warm events, Paleoceanography, 17, 4.1-4.10, 2002.

Schupbach, S., Fischer, H., Bigler, M., Erhardt, T., Gfeller, G., Leuenberger, D., Mini, O., Mulvaney, R., Abram, N. J., Fleet, L., Frey, M. M., Thomas, E., Svensson, A., Dahl-Jensen, D., Kettner, E., Kjaer, H., Seierstad, I., Steffensen, J. P., Rasmussen, S. O., Vallelonga, P., Winstrup, M., Wegner, A., Twarloh, B., Wolff, K., Schmidt, K., Goto-Azuma, K., Kuramoto, T., Hirabayashi, M., Uetake, J., Zheng, J., Bourgeois, J., Fisher, D., Zhiheng, D., Xiao, C., Legrand, M., Spolaor, A., Gabrieli, J., Barbante, C., Kang, J. H., Hur, S. D., Hong, S. B., Hwang, H. J., Hong, S., Hansson, M., Iizuka, Y., Oyabu, I., Muscheler, R., Adolphi, F., Maselli, O., McConnell, J., and Wolff, E. W.: Greenland records of aerosol source and atmospheric lifetime changes from the Eemian to the Holocene, Nat. Commun., 9, https://doi.org/10.1038/s41467-018-03924-3, 2018.

Scotese, C. R., Song, H., Mills, B. J. W., and van der Meer, D. G.: Phanerozoic paleotemperatures: The earth's changing climate during the last 540 million years, Earth-Sci. Rev., 215, https://doi.org/10.1016/j.earscirev.2021.103503, 2021.

Seki, O., Foster, G. L., Schmidt, D. N., Mackensen, A., Kawamura, K., and Pancost, R. D.: Alkenone and boron-based Pliocene pCO(2) records, Earth Planet. Sci. Lett., 292, 201–211, https://doi.org/10.1016/j.epsl.2010.01.037, 2010.

Sellers, W. D.: Global climatic model based on the energy balance of the Earth- Atmosphere system, J. Appl. Meteorol., 8, 392–400, 1969.

Shackleton, N. J.: The 100,000-year ice-age cycle identified and found to lag temperature, carbon dioxide, and orbital eccentricity, Science, 289, 1897–1902, https://doi.org/10.1126/science.289.5486.1897, 2000.

Shackleton, N. J. and Opdyke, N. D.: Oxygen isotope and palaeomagnetic evidence for early Northern Hemisphere glaciation., Nature, 270, 216–223, 1977.

Shackleton, N. J., Hall, M. A., and Vincent, E.: Phase relationships between millennial-scale events 64,000-24,000 years ago, Paleoceanography, 15, 565–569, https://doi.org/10.1029/2000pa000513, 2000.

Shaffer, G., Olsen, S. M., and Bjerrum, C. J.: Ocean subsurface warming as a mechanism for coupling Dansgaard-Oeschger climate cycles and ice-rafting events, Geophys. Res. Lett., 31, https://doi.org/10.1029/2004gl020968, 2004.

Stocker, T. F. and Johnsen, S. J.: A minimum thermodynamic model for the bipolar seesaw, Paleoceanography, 18, 11-1-11–9, 2003.

Svensson, A., Dahl-Jensen, D., Steffensen, J. P., Blunier, T., Rasmussen, S. O., Vinther, B. M., Vallelonga, P., Capron, E., Gkinis, V., Cook, E., Kjaer, H. A., Muscheler, R., Kipfstuhl, S., Wilhelms, F., Stocker, T. F., Fischer, H., Adolphi, F., Erhardt, T., Sigl, M., Landais, A., Parrenin, F., Buizert, C., McConnell, J. R., Severi, M., Mulvaney, R., and Bigler, M.: Bipolar volcanic synchronization of abrupt climate change in Greenland and Antarctic ice cores during the last glacial period, Clim. Past, 16, 1565–1580, https://doi.org/10.5194/cp-16-1565-2020, 2020.

Timmermann, A., Gildor, H., Schulz, M., and Tziperman, E.: Coherent resonant millennial-scale climate oscillations triggered by massive meltwater pulses, J. Clim., 16, 2569–2585, https://doi.org/10.1175/1520-0442(2003)016<2569:crmcot>2.0.co;2, 2003.

Turner, S. K.: Pliocene switch in orbital-scale carbon cycle/climate dynamics, Paleoceanography, 29, 1256–1266, https://doi.org/10.1002/2014pa002651, 2014.

Tziperman, E. and Gildor, H.: On the mid-Pleistocene transition to 100-kyr glacial cycles and the asymmetry between glaciation and deglaciation times, Paleoceanography, 18, https://doi.org/10.1029/2001pa000627, 2003.

Waelbroeck, C., Labeyrie, L., Michel, E., Duplessy, J. C., McManus, J. F., Lambeck, K., Balbon, E., and Labracherie, M.: Sea-level and deep water temperatures changes derived from benthic foraminifera isotopic records, Quat. Sci. Rev., 21, 295–305, 2002.

van de Wal, R. S. W., de Boer, B., Lourens, L. J., Koehler, P., and Bintanja, R.: Reconstruction of a continuous high-resolution CO2 record over the past 20 million years, Clim. Past, 7, 1459–1469, https://doi.org/10.5194/cp-7-1459-2011, 2011.

Wang, Y. J., Cheng, H., Edwards, R. L., An, Z. S., Wu, J. Y., Shen, C. C., and Dorale, J. A.: A high-resolution absolute-dated Late Pleistocene monsoon record from Hulu Cave, China, Science, 294, 2345–2348, https://doi.org/10.1126/science.1064618, 2001.

Westerhold, T., Marwan, N., Drury, A. J., Liebrand, D., Agnini, C., Anagnostou, E., Barnet, J. S. K., Bohaty, S. M., De Vleeschouwer, D., Florindo, F., Frederichs, T., Hodell, D. A., Holbourn, A. E., Kroon, D., Lauretano, V., Littler, K., Lourens, L. J., Lyle, M., Palike, H., Rohl, U., Tian, J., Wilkens, R. H., Wilson, P. A., and Zachos, J. C.: An astronomically dated record of Earth's climate and its predictability over the last 66 million years, Science, 369, 1383-+, https://doi.org/10.1126/science.aba6853, 2020.

Woillard, G.: Grande Pile Peat Bog : A Continuous Pollen Record for the Last 140,000 Years, Quat. Res., 9, 1–21, 1978.

Wolff, E. W., Chappellaz, J., Blunier, T., Rasmussen, S. O., and Svensson, A.: Millennial-scale variability during the last glacial: The ice core record, Quat. Sci. Rev., 29, 2828–2838, https://doi.org/10.1016/j.quascirev.2009.10.013, 2010.

Zachos, J., Pagani, M., Sloan, L., Thomas, E., and Billups, K.: Trends, rhythms, and aberrations in global climate 65 Ma to present, Science, 292, 686–693, 2001.

Zagwijn, W. H.: Vegetation and climate during warmer intervals in the Late Pleistocene of western and central Europe., Quat. Internatonal, 3/4, 57-67., 1989.

Zhang, S., Wang, X., Hammarlund, E. U., Wang, H., Costa, M. M., Bjerrum, C. J., Connelly, J. N., Zhang, B., Bian, L., and Canfield, D. E.: Orbital forcing of climate 1.4 billion years ago, Proc. Natl. Acad. Sci. U. S. A., 112, E1406–E1413, https://doi.org/10.1073/pnas.1502239112, 2015.

Ziemen, F. A., Kapsch, M.-L., Klockmann, M., and Mikolajewicz, U.: Heinrich events show two-stage climate response in transient glacial simulations, Clim. Past, 15, 153–168, https://doi.org/10.5194/cp-15-153-2019, 2019.

Figure captions

Figure 1. Earth Climate history represented by two marine records and an ice core one. (a) Record of benthic $\delta^{18}O$ of the CENOGRID stack for the last 66 Myr; the hot, warm, cool, and icehouse intervals, after Westerhold et al. (2020), are indicated along the abscissa. (b) Benthic $\delta^{18}O$ record of the U1308 marine core (Hodell and Channell, 2016) for the last 3.2 Myr; the 40 kyr, 100 kyr, and Mid-Pleistocene transition (MPT) intervals are indicated along the top of the diagram. (c) 122 ka b2k $\delta^{18}O$ of the NGRIP ice core (Rasmussen et al., 2014) for the last 122 kyr b2k. Here 'b2k' means before 2000 A.D.

Figure 2. Recurrence analysis of the $\delta^{18}O$ record in U1308 *Cibicidoides sp.* (Hodell and Channell, 2016). (a) Recurrence plot (RP); the proximity threshold is $\Delta(\delta^{18}O)$ = 0.2 per mil. (b) Time series of the *Cibicidoides sp.* $\delta^{18}O$ (blue curve, top) and of the bulk carbonate $\delta^{18}O$ (magenta curve, bottom); (c) recurrence rate (RR) with significant values labeled with a red cross, and RR close to the threshold in pink . Vertical bars represent the major transitions (5+1) determined by the analysis. The RP web site is http://www.recurrence-plot.tk/.

Figure 3. Recurrence analysis of U1308 bulk carbonate $\delta^{18}O$ (Hodell and Channell, 2016). (a) RP of the bulk carbonate $\delta^{18}O$, with the same proximity threshold as in Fig. 2A. (b) same as Fig. 2B. (c) same as in Fig. 2c except that the vertical bars now represent the major thresholds (4+3) determined by the RR analysis in Fig. 3c. The RP web site is http://www.recurrence-plot.tk/.

Figure 4. Recurrence analysis of NGRIP $\delta^{18}O$. (a) NGRIP $\delta^{18}O$ variations over the last 122 kyr b2k (Rasmussen et al., 2014); selected canonical Dansgaard-Oeschger (DO) events are indicated on the abscissa by the numbers assigned by Dansgaard et al. (1993). (b) RP of the time series in panel (A) above; the proximity threshold here is $\Delta(\delta^{18}O)$= 1.3 per mil). (c) Recurrence rate analysis showing the selected thresholds (7+7) indicated by the vertical bars The RP web site is http://www.recurrence-plot.tk/.

Figure 5. Recurrence analysis of NGRIP $\delta^{18}O$. (a) NGRIP $\delta^{18}O$ variations over the last 122 kyr b2k (Rasmussen et al., 2014); same as in Fig. 4a. (b) same as in Fig. 4b. (c) Variation of the sea level over the last 122 kyr BP, as reconstructed from benthic $\delta^{18}O$ foraminifera by Waelbroeck et al. (2002); bold red line is the global mean sea level (m) below present, and light blue lines are the minimum and maximum global mean sea level values (m) below present. Horizontal green line segments indicate some key sea levels. The RP web site is http://www.recurrence-plot.tk/.

Figure 6. Bond cycles. (a) Idealized Bond cycle as illustrated after Alley (1998) DO: Dansgaard-Oeschger event, H event: Heinrich event, NADW: North Atlantic Deep Water. (b)Variations in the percentage of *Neogloboquadrina pachyderma* (s.), a species indicative of cold surface water, from DSDP 609 (Bond et al., 1992), illustrating two Bond cycles. These cycles show a series of Dansgaard-Oeschger (DO) cycles composed of an abrupt warming that is followed by a return to glacial conditions represented by "stadials." Every Bond

cycle corresponds to a long-term cooling trend that starts with a strong warming and ends with a stadial that includes a massive iceberg discharge into the North Atlantic; the latter Heinrich events (HEs) are marked by a letter 'H', followed by a number assigned by Bond et al. (Bond et al., 1992)).

Figure 7. Schematic diagram of the proposed, updated Bond cycle. (a) The amended scheme here differs from the one in Fig. 6a by adding the IRD event associated to every Greenland stadials (GS). The canonical DO are labeled here Greenland interstadials (GI). (b) The revised cycle here differs from the one in Fig. 6a by using the NGRIP $\delta^{18}O$ data (Rasmussen et al., 2014) to mark the GSs and GI.. IRD events observed in contemporaneous marine records by Bond and Lotti (1995), are indicated by the letters 'f' to "h" while IRD events that were observed but not assigned a number also by Bond and Lotti (1995), are indicated by a letter 'x'. HE numbers as in Fig. 5. (b) Maps illustrating the climate evolution associated with the "Long-Term Cooling Trend" that corresponds to a Bond cycle in panel (A) above; the last DO cycle, named a Heinrich Stadial, is characterized by a massive release of icebergs. Annual mean SST (°C) for a GI (here 47 ka), a GS (here 44.4 ka), and a Heinrich stadial (here 48 ka), as simulated in a transient experiment of MIS3 (Menviel et al., 2014, 2021). GIS = Greenland Ice Sheet, LIS = Laurentide Ice Sheet, BIS = British Isles Ice Sheet, and FIS = Fenno-Scandian Ice Sheet.

Table captions

Table 1. Statistics of the recurrence rate analysis for U1308 benthic $\delta^{18}O$, U1308 bulk carbonate $\delta^{18}O$ (Hodell and Channell, 2016) and NGRIP $\delta^{18}O$ (Rasmussen et al., 2014). The RR prominence higher than RR standard deviation are considered as major transitions and labeled with a red cross on Figs. 2a, 3a and 4c. RR prominence slightly lower to the standard variation are identified with an asterisk and labeled with pink cross on the same figures. RR prominence significance: # above the standard deviation (sd), $ slightly lower than the standard deviation.

Table 2. Comparison of the main steps detected by Hodell and Channell (2016) from U1308 marine record with those deduced from the Recurrence Plot of the benthic $\delta^{18}O$ and bulk carbonate $\delta^{18}O$ data of the same record. RR prominence significance as in Tab. 1

Table 3. Thresholds identified in the recurrence plot of NGRIP $\delta^{18}O$ record and their correspondence in the marine isotope stratigraphy of the last climate cycle stratigraphy (Bassinot et al., 1994; Lisiecki and Raymo, 2005). RR prominence significance as in Tab. 1

Supplementary material

Suppl. Fig. 1. Detection of the major transitions in U1308 benthic $\delta^{18}O$ record (Hodell and Channell, 2016) using the KS augmented test by Bagniewski et al. (2021). The identified transitions correspond to the various boundaries between the marine isotope stages (MIS) determined during the past 3.2 Myr. In blue cooling transitions and in red warming transitions. The MIS labels are according to Lisiecki & Raymo (2005) while substage numbering if from Railsback et al. (2015).

Suppl. Fig. 2. Detection of abrupt transitions in the NGRIP $\delta^{18}O$ record (Rasmussen et al., 2014)using the KS augmented test by Bagniewski et al. (2021).. In dark gray, Greenland interstadials, labeled for example GI-3, or Greenland interstadial "warm" substages labeled for example GI-8c. Greenland interstadial "cold" substages are in light gray. Events labeled in green or the greenbox indicate a disagreement between Rasmussen et al. (2014) interpretation and the KS test results. The red question marks are event not labeled in Rasmussen et al. (2014)

Suppl. Fig. 3. Scatter plots a) of the DO duration (in yr b2k) versus the DO number; b) of DO relative sea-level variation (in m) versus DO duration (in yr b2k). The DO relative sea-level values are estimated from Waelbroeck et al. (2002) for the DO boundaries given by Rasmussen et al. (2014)

Suppl. Tab. 1. Duration of the DO cycles as estimated from the NGRIP $\delta^{18}O$ boundaries from Rasmussen et al. (2014)

References

Bagniewski, W., Ghil, M., and Rousseau, D. D.: Automatic detection of abrupt transitions in paleoclimate records, Chaos, in press, 2021.

Hodell, D. A. and Channell, J. E. T.: Mode transitions in Northern Hemisphere glaciation: co-evolution of millennial and orbital variability in Quaternary climate, Clim. Past, 12, 1805–1828, https://doi.org/10.5194/cp-12-1805-2016, 2016.

Lisiecki, L. E. and Raymo, M. E.: A Pliocene-Pleistocene stack of 57 globally distributed benthic delta O-18 records, Paleoceanography, 20, PA1003, doi:10.1029/2004PA001071, 2005.

Railsback, L. B., Gibbard, P. L., Head, M. J., Voarintsoa, N. R. G., and Toucanne, S.: An optimized scheme of lettered marine isotope substages for the last 1.0 million years, and the climatostratigraphic nature of isotope stages and substages, Quat. Sci. Rev., 111, 94–106, https://doi.org/10.1016/j.quascirev.2015.01.012, 2015.

Rasmussen, S. O., Bigler, M., Blockley, S. P., Blunier, T., Buchardt, S. L., Clausen, H. B., Cvijanovic, I., Dahl-Jensen, D., Johnsen, S. J., Fischer, H., Gkinis, V., Guillevic, M., Hoek, W. Z., Lowe, J. J., Pedro, J. B., Popp, T., Seierstad, I. K., Steffensen, J. P., Svensson, A. M., Vallelonga, P., Vinther, B. M., Walker, M. J. C., Wheatley, J. J., and Winstrup, M.: A stratigraphic framework for abrupt climatic changes during the Last Glacial

period based on three synchronized Greenland ice-core records: refining and extending the INTIMATE event stratigraphy, Quat. Sci. Rev., 106, 14–28, https://doi.org/10.1016/j.quascirev.2014.09.007, 2014.

Waelbroeck, C., Labeyrie, L., Michel, E., Duplessy, J. C., McManus, J. F., Lambeck, K., Balbon, E., and Labracherie, M.: Sea-level and deep water temperatures changes derived from benthic foraminifera isotopic records, Quat. Sci. Rev., 21, 295–305, 2002.

Fig. 1

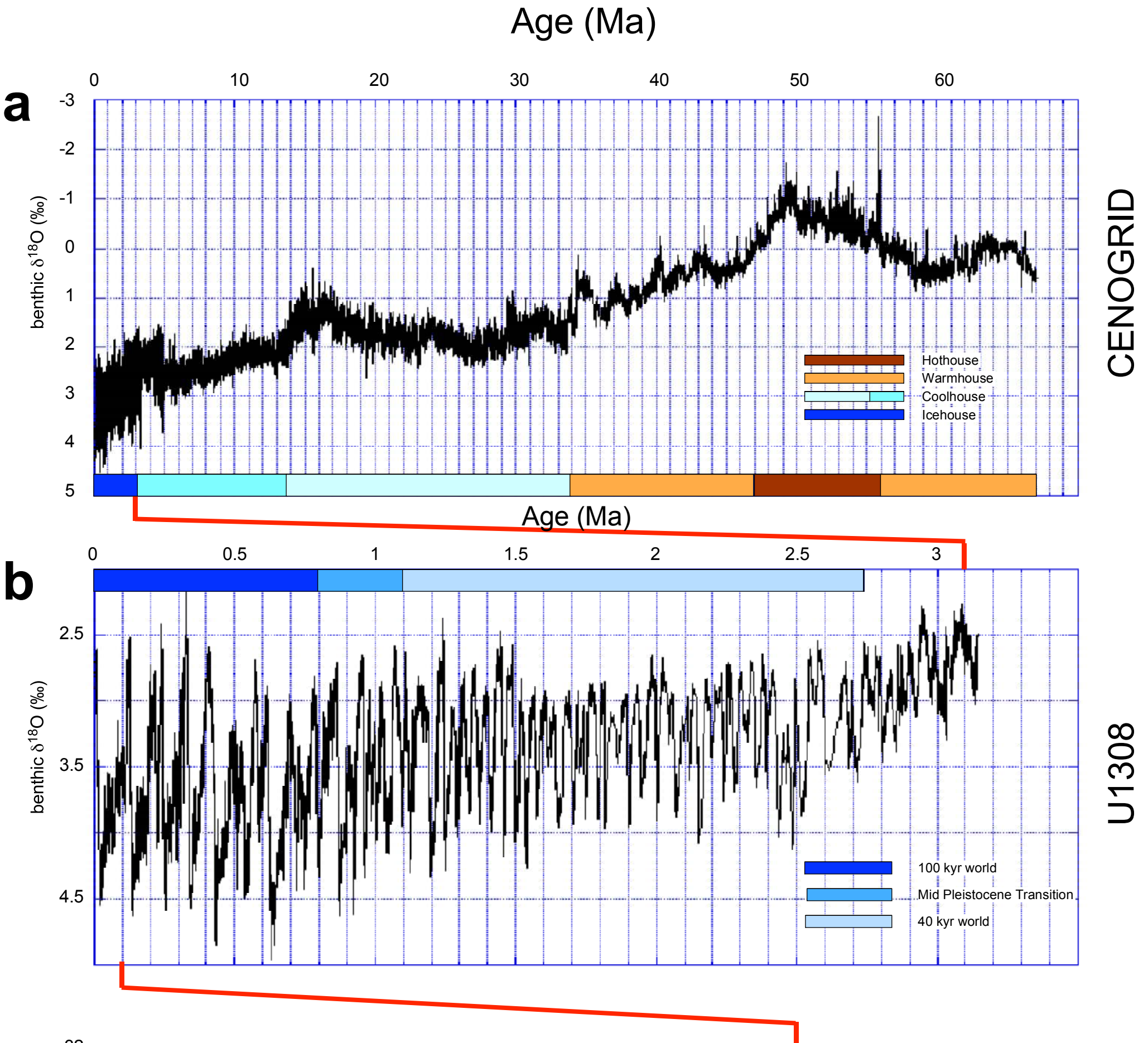
Age (Ma)
a
benthic δ18O (‰)
CENOGRID
Hothouse
Warmhouse
Coolhouse
Icehouse
Age (Ma)
b
benthic δ18O (‰)
U1308
100 kyr world
Mid Pleistocene Transition
40 kyr world
c
δ18O (‰)
NGRIP
Age (ka b2k)

Fig. 2

Recurrence U1308 benthic $\delta^{18}0$

Age (ka BP)

a

δ^{18}O bulk carb. (PDB)

Cibicidoides sp. δ^{18}O (VPDB)

b

Age (ka BP)

c

Recurrence Rate

Age (ka BP)

Fig. 3

Recurrence U1308 bulk carbonate $\delta^{18}0$

Age (ka BP)

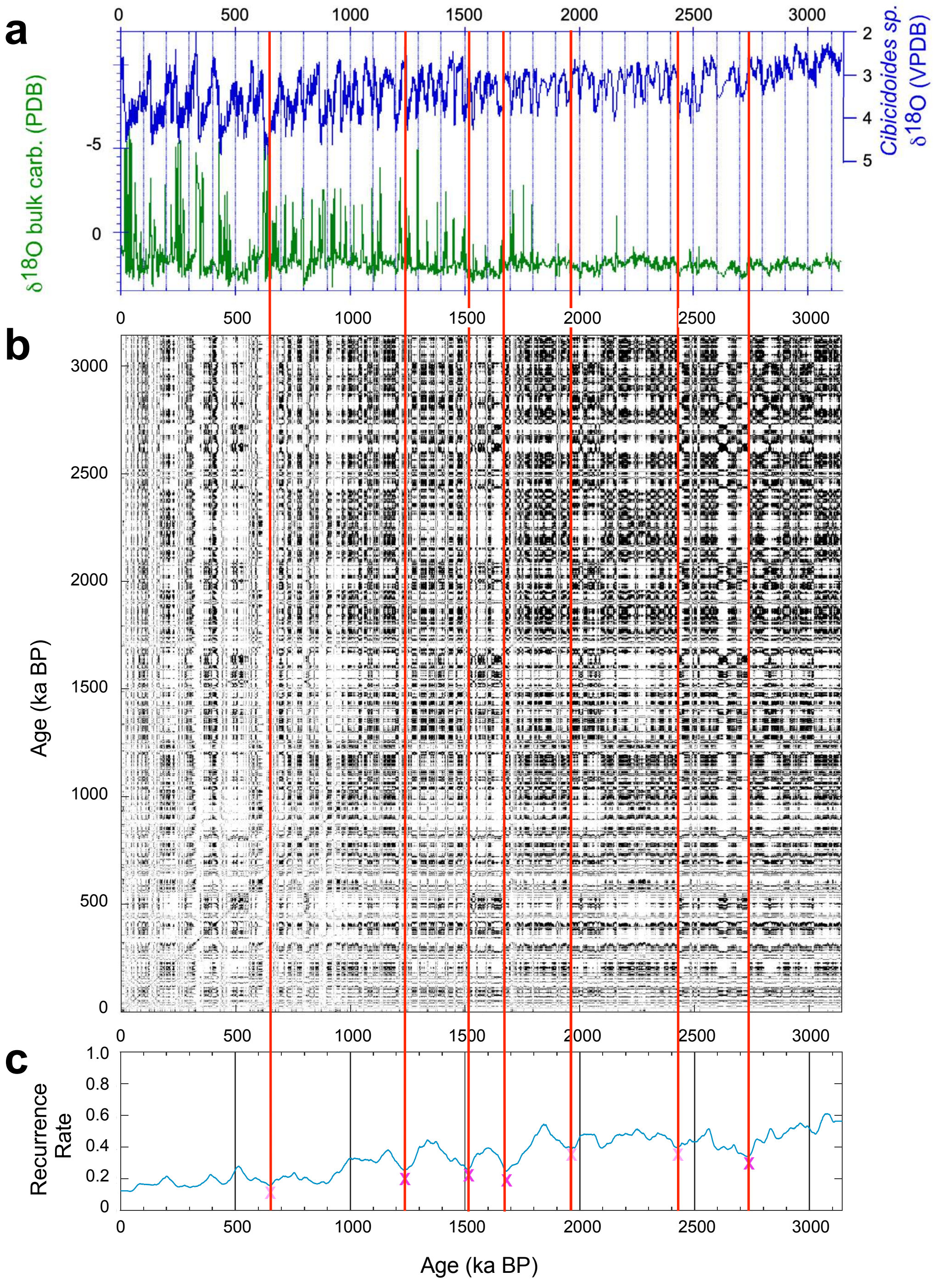

Fig. 4

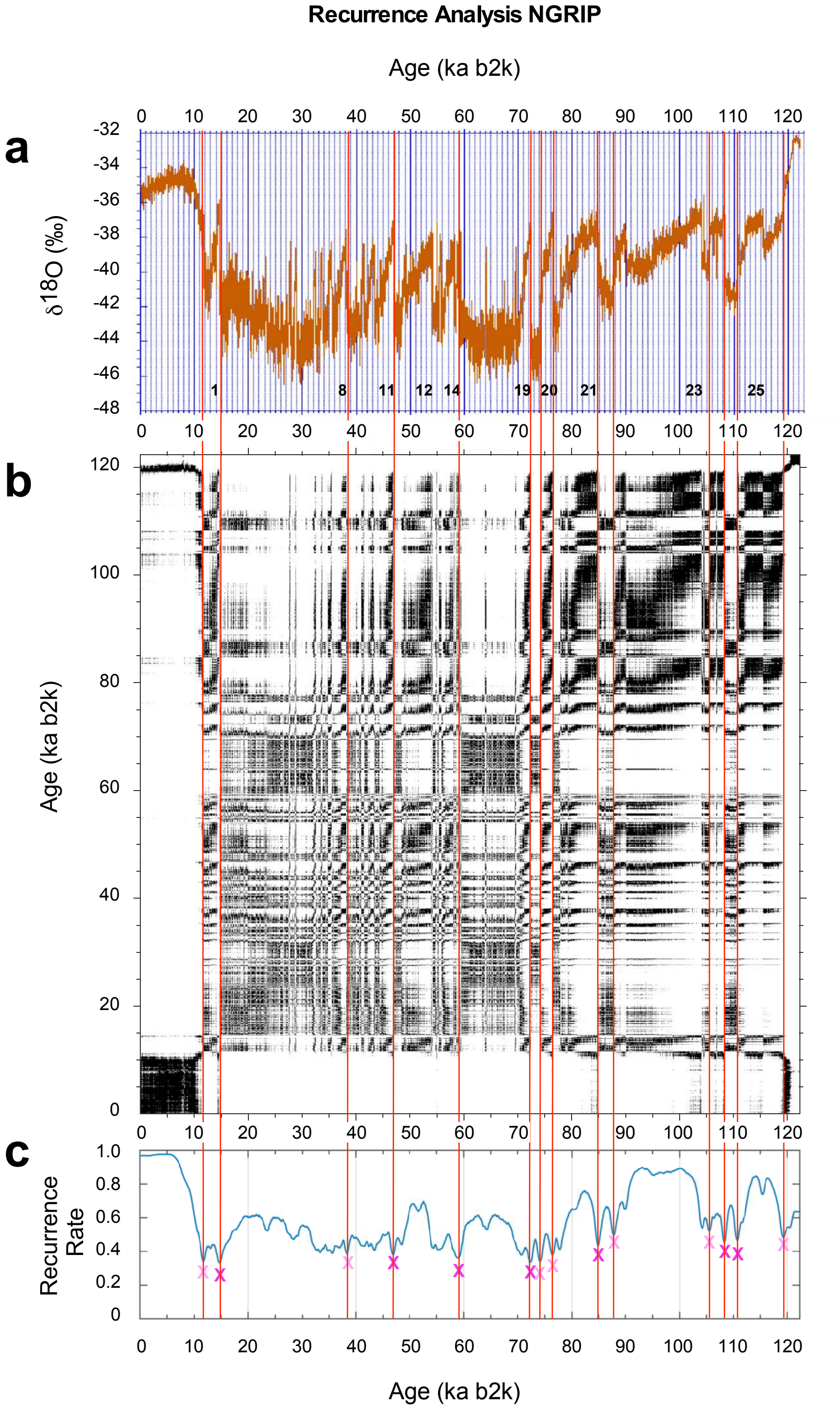
Recurrence Analysis NGRIP
a
Age (ka b2k)
δ18O (‰)
-32
-34
-36
-38
-40
-42
-44
-46
-48
0
10
20
30
40
50
60
70
80
90
100
110
120
1
8
11
12
14
19
20
21
23
25
b
Age (ka b2k)
120
100
80
60
40
20
0
c
Recurrence Rate
1.0
0.8
0.6
0.4
0.2
0
Age (ka b2k)

Fig. 5

Recurrence Analysis NGRIP

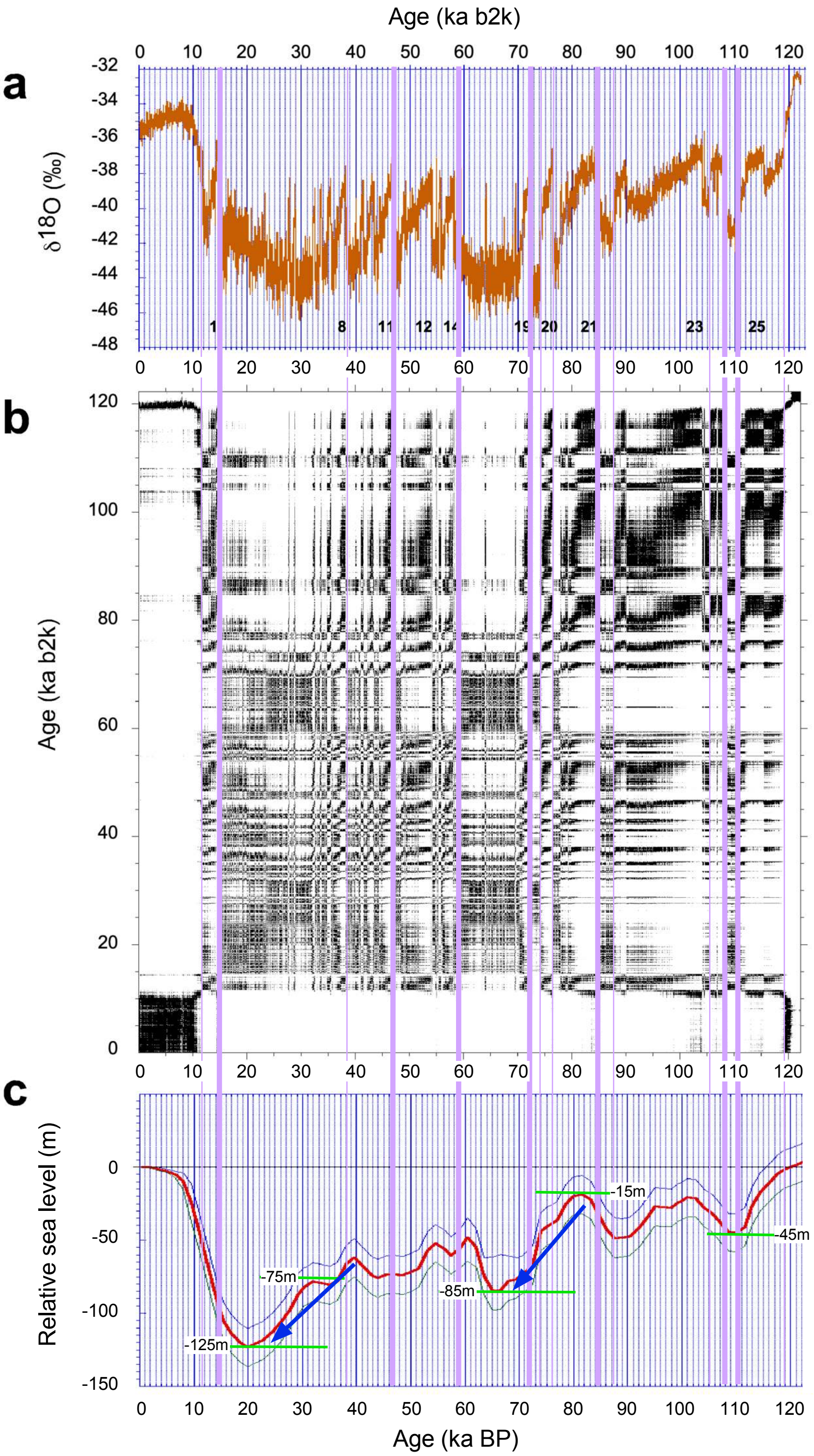

Fig.6

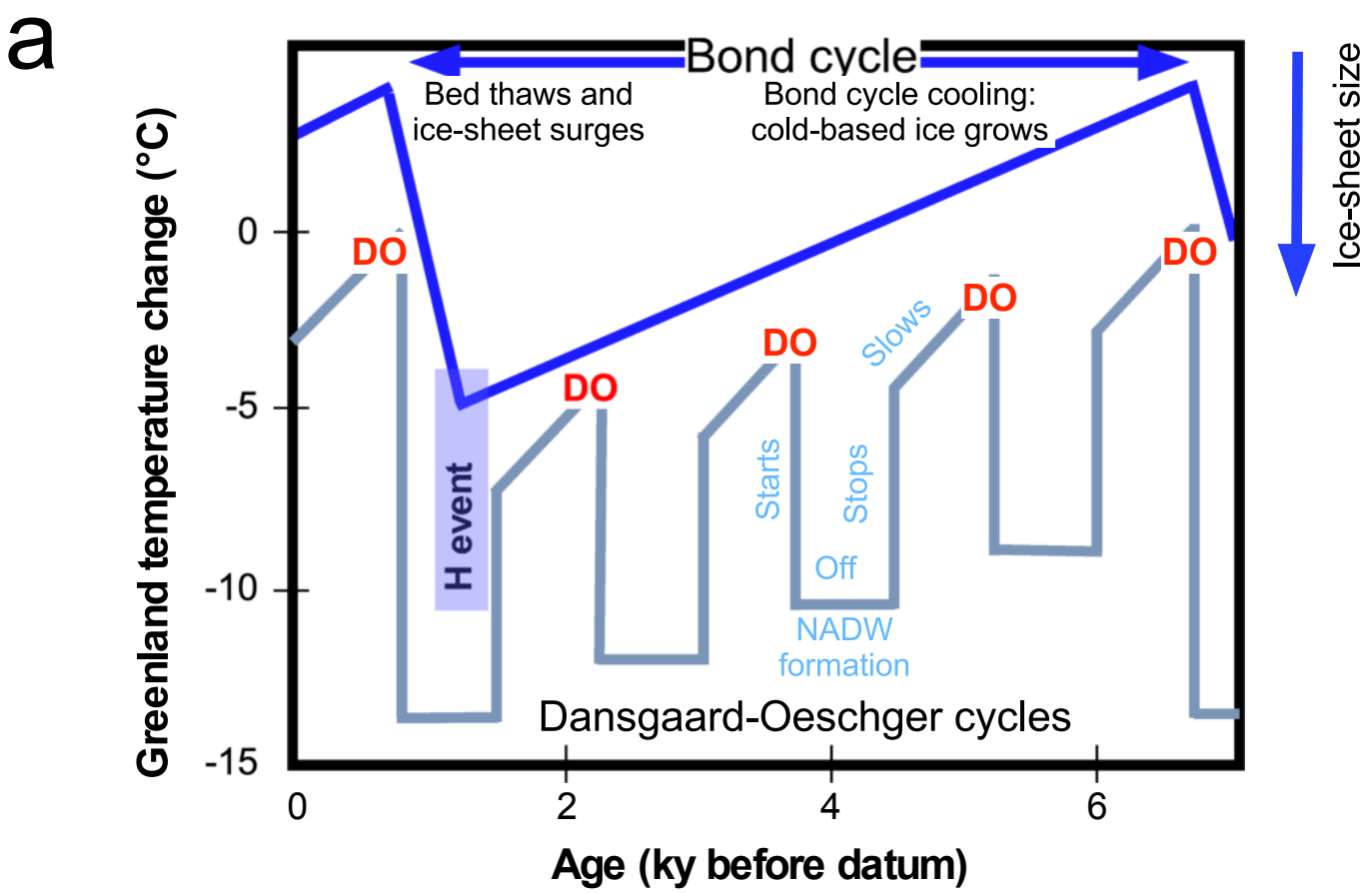
a
Bond cycle
Bed thaws and ice-sheet surges
Bond cycle cooling: cold-based ice grows
Ice-sheet size
Greenland temperature change (°C)
0
-5
-10
-15
DO
H event
Starts
Slows
Stops
Off
NADW formation
Dansgaard-Oeschger cycles
0
2
4
6
Age (ky before datum)

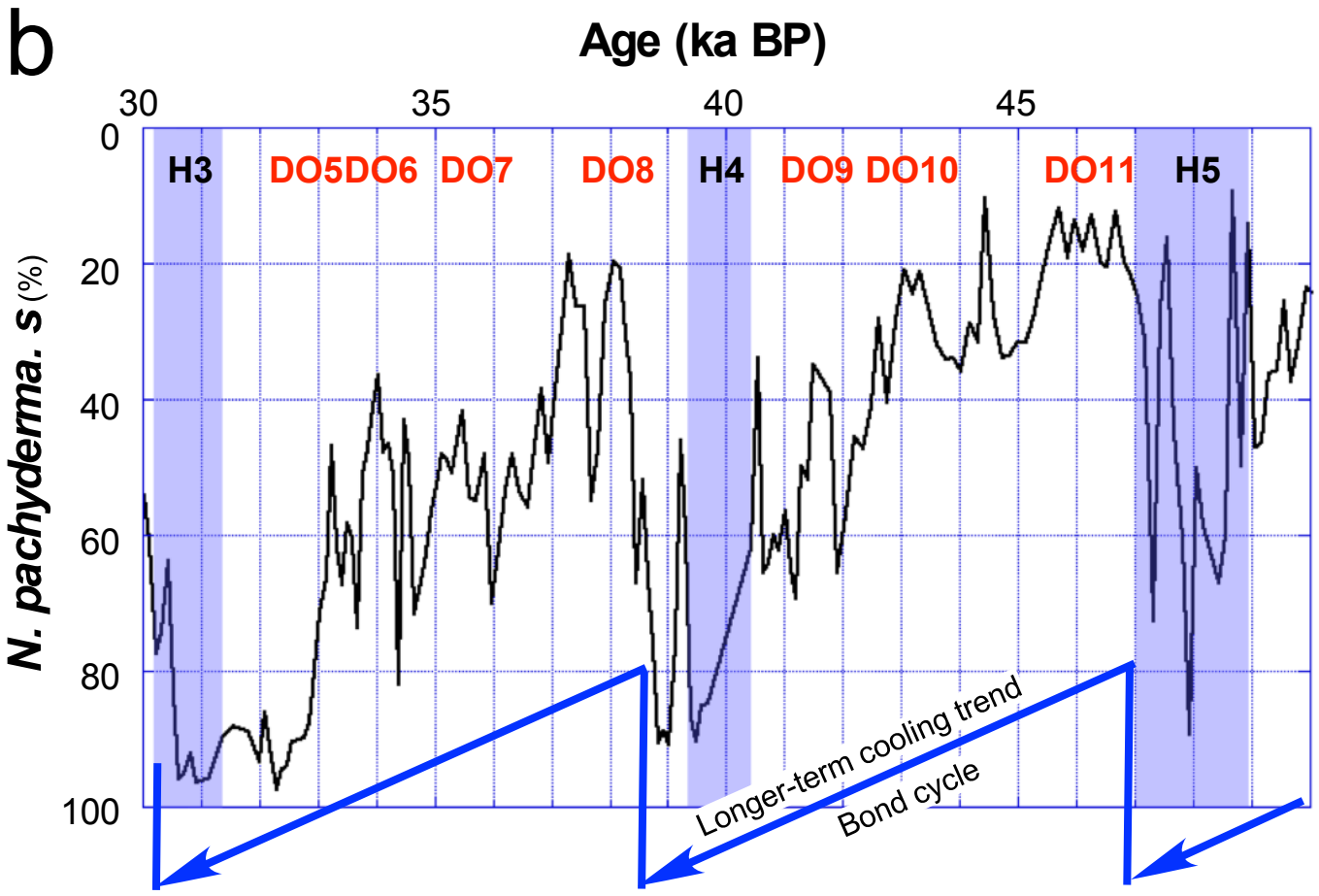
b
Age (ka BP)
30
35
40
45
0
20
40
60
80
100
N. pachyderma. s (%)
H3
DO5DO6
DO7
DO8
H4
DO9 DO10
DO11
H5
Longer-term cooling trend
Bond cycle

Fig. 7

a

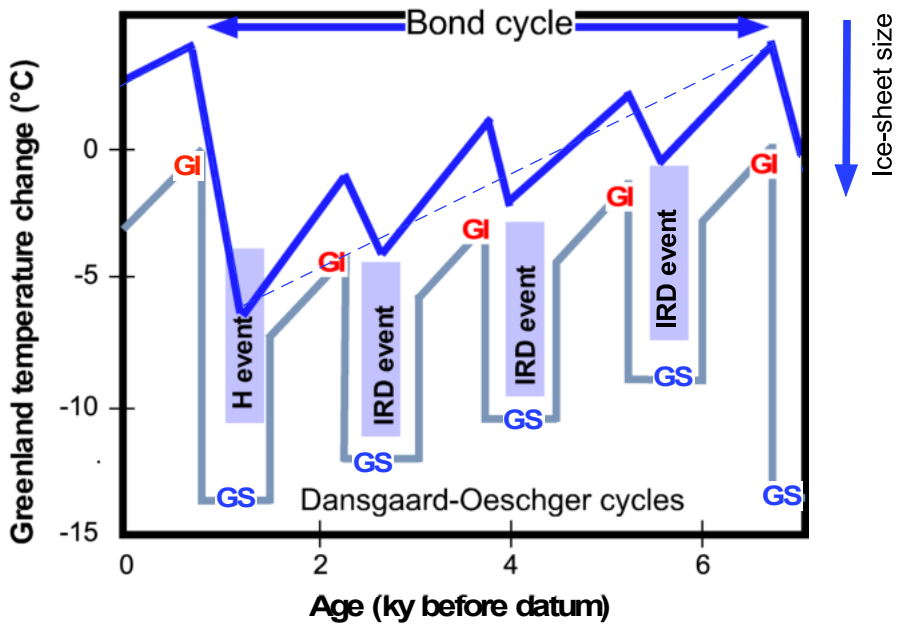

b

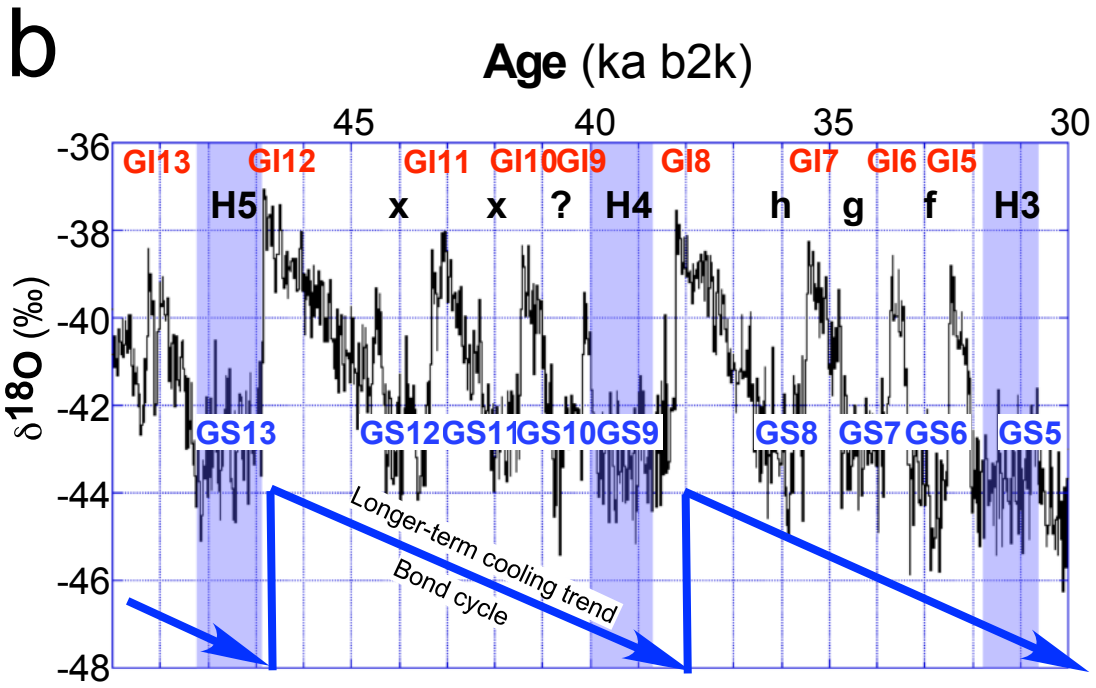

c

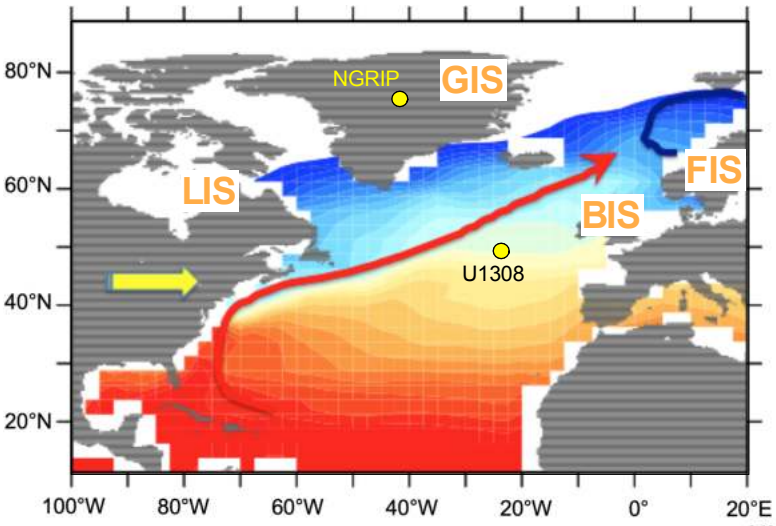

Greenland Interstadial

N Atlantic westerlies increase
Sea ice decreases
Salt transport to NA
-> NADW strenghens
Re-growth of NH ice sheets

High Ice shelves destabilization (high decrease in elevation) through subsurface warming
Strong NH ice sheets Ice streaming 'HE)
Sea ice increases
-> NADW weakens

NH ice sheets destabilize (low decrease in elevation) through subsurface warming
Ice streaming increases
Sea ice increases (IRDs)
-> NADW weakens

N Atlantic westerlies increase
Sea ice decreases
Salt transport to NA
-> NADW strenghens
Re-growth of NH ice sheets

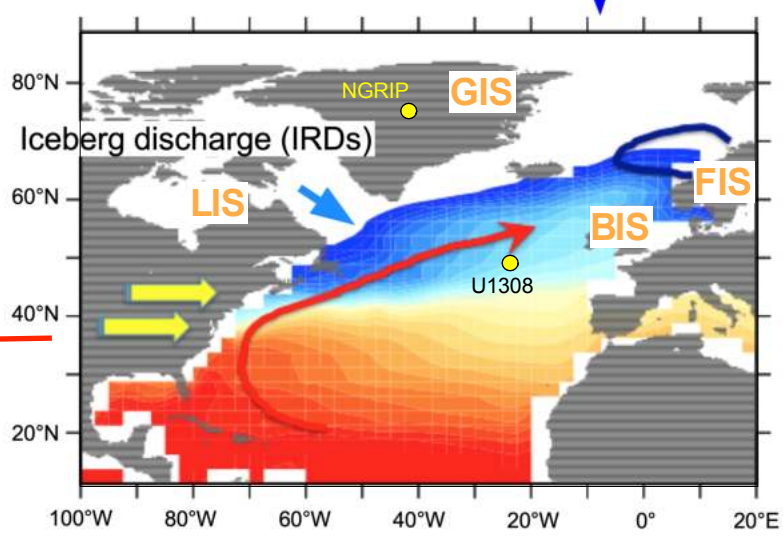

Greenland Stadial

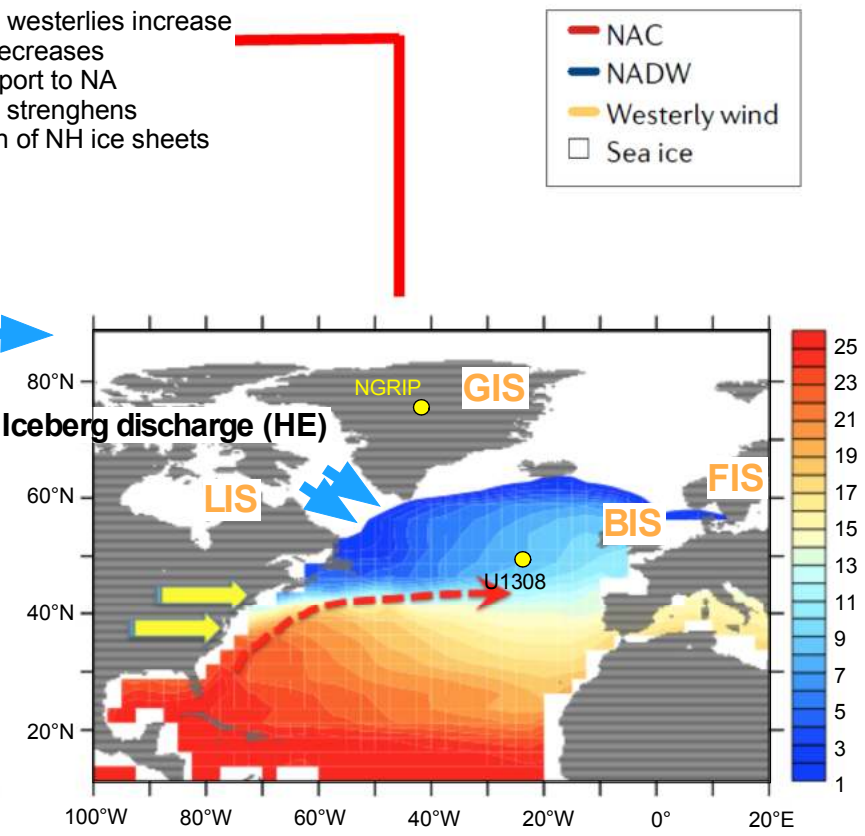

Heinrich Stadial

Supp. Fig.1

Detection of Abrupt transitions from benthic $\delta^{18}O$ in U1308 with the K-S method

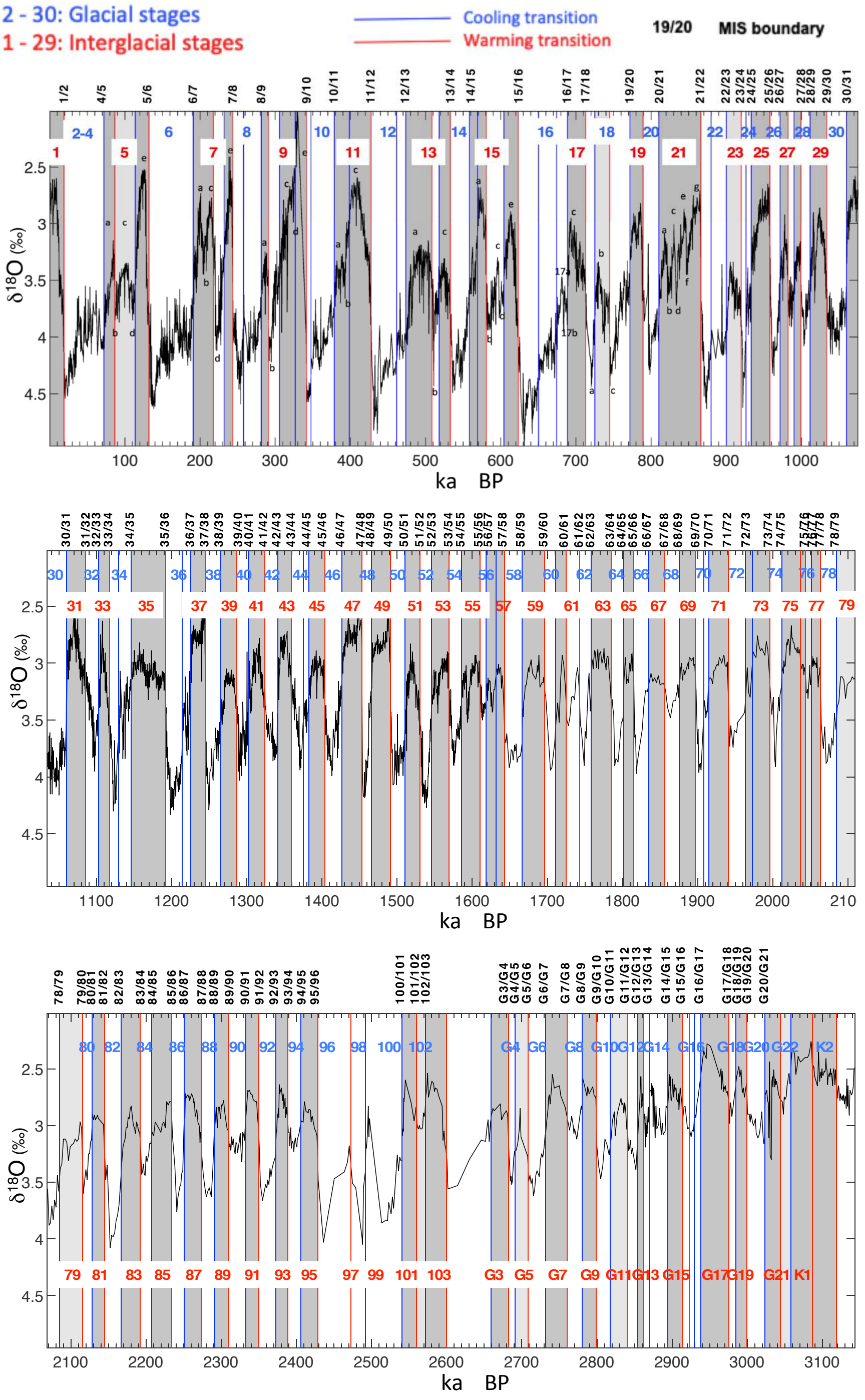

MIS boundaries from Lisiecki & Raymo (2005). Paleoceanography, PA1003, doi:10.1029/2004PA001071 and odd MIS from Hodell and Channel (2016) Climate of the Past, 12, https://doi.org/10.5194/cp-12-1805-2016.
Substage numbering from Railsback et al. (2015). Quaternary Science Reviews 111. https://doi.org/10.1016/j.quascirev.2015.01.012.

Supp. Fig. 2

Detection of Abrupt transitions in NGRIP d180 with the K-S method

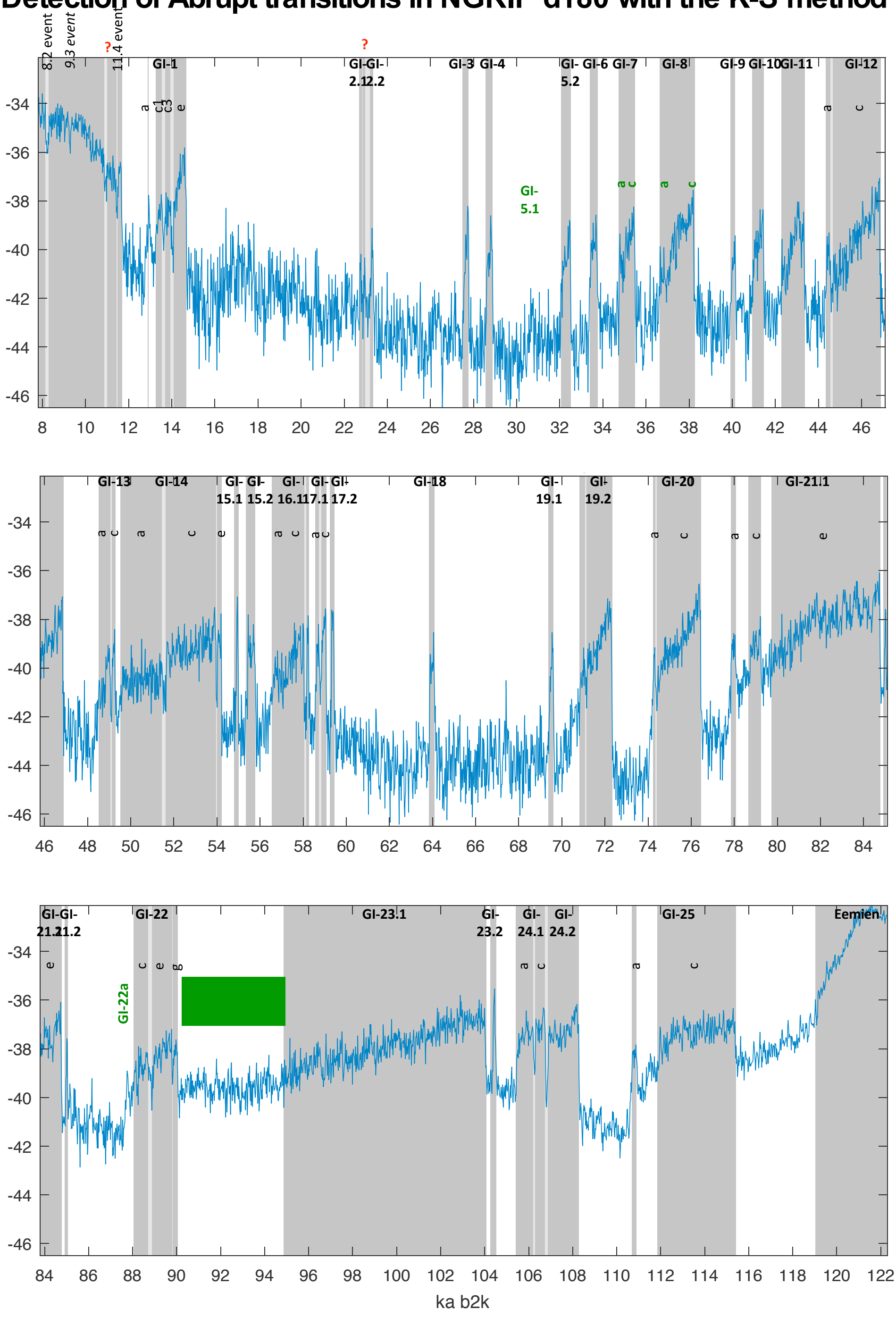

Supp. Fig. 3

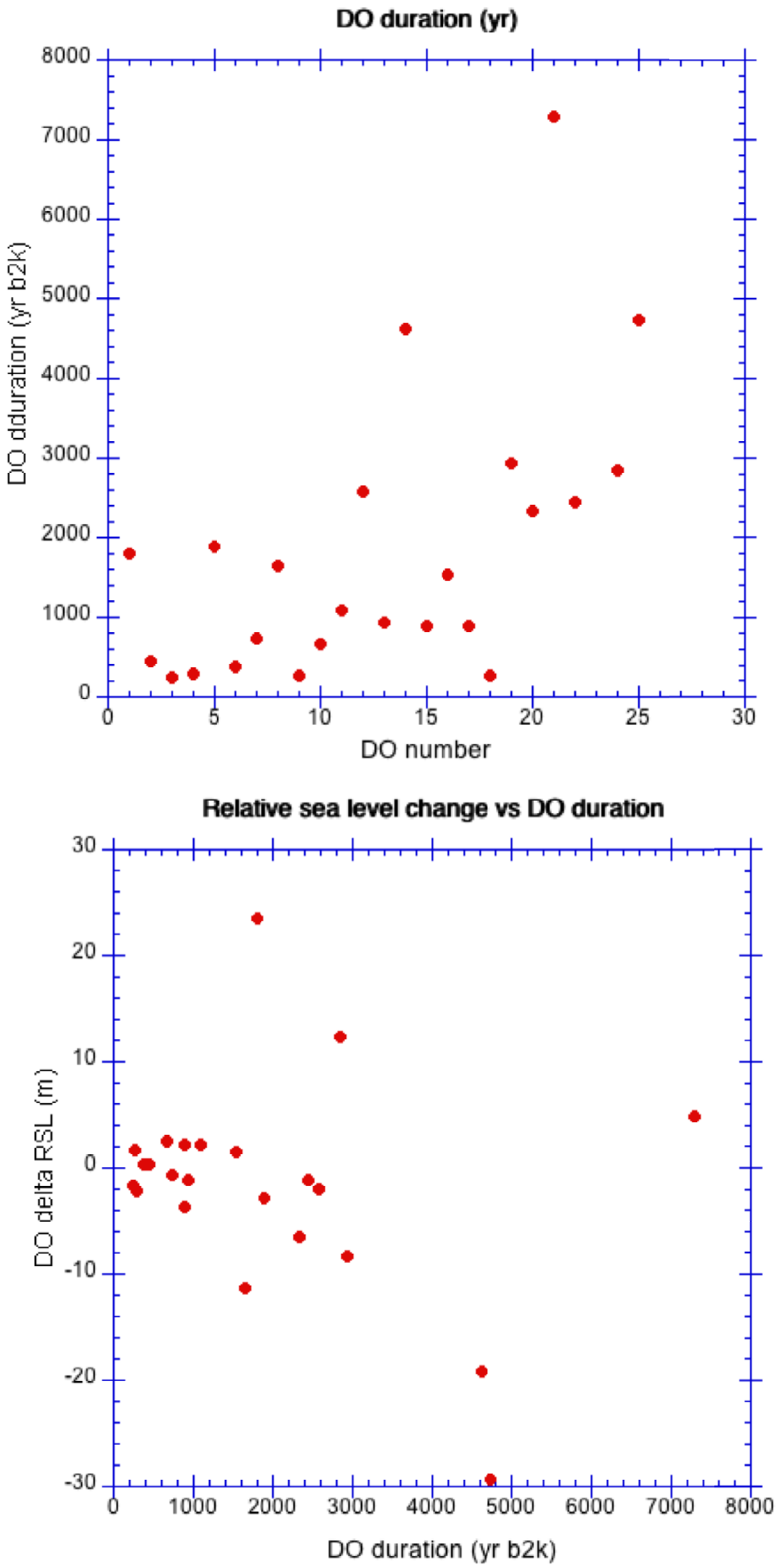
DO duration (yr)
DO dduration (yr b2k)
8000
7000
6000
5000
4000
3000
2000
1000
0
0
5
10
15
20
25
30
DO number
Relative sea level change vs DO duration
DO delta RSL (m)
30
20
10
0
-10
-20
-30
0
1000
2000
3000
4000
5000
6000
7000
8000
DO duration (yr b2k)